Detection and Classification of Lung Diseases Infected by Covid-19 Using FLICM Segmentation and HOG Feature-Based SCA-ELM Model

Tizita Asfaw Admassie

A Thesis Submitted to

The Department of Electronics and Communication Engineering

School of Electrical Engineering and Computing

Presented in Partial Fulfillment of the Requirement for the Degree of Master of Science in Electronics and Communication Engineering (Specialization in Communication Engineering)

Office of Graduate Studies

Adama Science and Technology University

June, 2022

Adama, Ethiopia

Detection and Classification of Lung diseases infected by covid-19 using FLICM segmentation and HOG feature based SCA-ELM model

Tizita Asfaw Admassie

Advisor: Dr. Satyasis Mirshra

A Thesis Submitted to

The Department of Electronics and Communication Engineering

School of Electrical Engineering and Computing

Presented in Partial Fulfillment of the Requirement for the Degree of Master of Science in Electronics and Communication Engineering (Specialization in Communication Engineering)

Office of Graduate Studies

Adama Science and Technology University

June, 2022

Adama, Ethiopia

Declaration

I hereby declare that this Master Thesis entitled "**Detection and Classification of Lung Diseases Infected by covid-19 using FLICM Segmentation and HOG Feature-based SCA-ELM Model"** is my original work. That is, it has not been submitted for the award of any academic degree, diploma, or certificate in any other university. All sources of materials that are used for this thesis have been duly acknowledged through citation

________________________	______________________	_______________
Name of student	Signature	Date

Recommendation

We, the advisors of this thesis, hereby certify that we have read the revised version of the thesis entitled "**Detection and Classification of Lung diseases infected by covid-19 using FLICM segmentation and HOG feature based SCA-ELM model**" prepared under our guidance Tizita Asfaw Admassie submitted in partial fulfillment of the requirements for the degree of Master's of Science in Electronics and Communication Engineering (Specialization in Communication Engineering). Therefore, we recommend the submission of revised version of the thesis to the department following the applicable procedures.

Major Advisor	Signature	Date
Co-advisor	Signature	Date

Approval Page for M.Sc. Thesis

We, the advisors of the thesis entitled "**Detection and Classification of Lung diseases infected by covid-19 using FLICM segmentation and HOG feature based SCA-ELM model**" and developed by Tizita Asfaw, hereby certify that the recommendation and suggestions made by the board of examiners are appropriately incorporated into the final version of the thesis.

Major Advisor	Signature	Date
Co-advisor	Signature	Date

We, the undersigned, members of the Board of Examiners of the thesis by Tizita Asfaw have read and evaluated the thesis entitled "**Detection and Classification of Lung diseases infected by covid-19 using FLICM segmentation and HOG feature based SCA-ELM model**" and examined the candidate during open defense. This is, therefore, to certify that the thesis is accepted for partial fulfillment of the requirement of the degree of Master of Science in Electronics and Communication Engineering (Specialization in Communication Engineering).

Chairperson	Signature	Date
Internal Examiner	Signature	Date
External Examiner	Signature	Date

Final approval and acceptance of the thesis is contingent upon submission of its final copy to the Office of Postgraduate Studies (OPGS) through the Department Graduate Council (DGC) and School Graduate Committee (SGC).

Department Head	Signature	Date
School Dean	Signature	Date
Office of Postgraduate Studies, Dean	Signature	Date

ACKNOWLEDGMENT

Above all, I would like to praise, honor and glorify the Almighty God for giving me the opportunity, strength, peace, and health to successfully complete this piece of work and for the inexorable support in my overall life.

I would like to express my very great appreciation to Dr. Satyasis Mishra and Dr. Dereje Teklu, my research advisors, for his patient guidance, enthusiastic encouragement and useful critiques of this research work. Their willingness to give their time so generously has been very much appreciated.

I would like to express my deep gratitude toward my family for their support & the encouragement which helped me in completing this paper.

Table of Contents

List of Figures

List of Tables

List of Acronyms

SCA	Sine Cosine Algorithm
HOG	Histogram oriented Graph
FLICM	Fuzzy Local Information C Means
ELM	Extreme Learning Machine
ML	Machine Learning
AI	Artificial Intelligence
ARDS	Acute Respiratory Distress Syndrome
CNN	Convolutional Neural Network
DNN	Deep Neural Network
CBC	Complete Blood Count
ICNN	Improved Convolutional Neural Network
CT	Computed Tomography
PA	Posterior-Anterior
FRFLICM	Fast and robust Fuzzy Local Information C Means
EnFCM	Enhanced Fuzzy C Means Algorithm
RBFNN	Radial Basis Function Neural Network
SVM	Support Vector Machine
MERS	Middle East Respiratory Syndrome
CDC	Disease Control and Prevention
WHO	World Health Organization
MSCA	Modified Sine Cosine Algorithm
SSIM	Structured Similarity Index
RVM	Relevance Vector Machine
BRIEF	Binary Robust Independent Elementary Features
FAST	Features from Accelerated Segment Tree
ORB	Oriented FAST and Rotated BRIEF
WCO	WHO Country office
SARS	Severe Acute Respiratory Infected Syndrome

NIAID	National Institute for Allergy and Infectious
PSO	Particle Swarm Optimization
APSO	Adaptive Particle Swarm Optimization
MSE	Mean Square Error
PSNR	Peak Signal-to-Noise Ratio
RBF	Radial Basis Function
GRBF	Gaussian Radial Basis Function

ABSTRACT

Medical imaging achieves enormous claims on automated, reliable, and efficient diagnosis in all medical-related issues. During the present pandemic situation of covid-19, enormous numbers of people are affected by lung diseases. Lung infections are evolved as different types of diseases. It is a problematic task for a clinical physician to segment, detect, and extract infected areas of the lung due to covid-19 and classify the type of infection and its stage from X-ray images. During the present pandemic situation of covid-19, enormous peoples are affected with lungs diseases. Lung infections are evolved as different types of diseases. It is a tough and multifarious the medical practitioner to segment, detect, and extract infected areas of lung due to covid-19 and classify the type of infection and its stage from X-ray images. The size, shape, and position of infection differ from dissimilar patient's lung. Several efforts have been proposed for image detection and classification in the literature by considering machine learning and deep learning models. Motivated by the advancement of machine learning for classification of lung diseases, we are proposing a novel segmentation technique and a classifier for detection and classification of lung diseases.

This research suggests a HOG (Histogram oriented Graph) feature based hybrid modified SCA (Sine Cosine Algorithm)-Extreme Learning Machine model to classify different infected and non-infected lung diseases related to COVID-19. An image enhancement technique also suggested by utilizing Modified Sine Cosine (MSCA) optimization to increase the quality of images. Further, a new Fast and robust Fuzzy Local Information C Means (FRFLICM) segmentation technique for detection of lung infection from X-ray images that can inform radiologist and doctors about the details of lung infection due to covid-19. The lungs chest X-ray images are collected from different hospitals of Ethiopia and Kaggel website. The quality measures SSIM and PSNR are considered for image segmentation and achieved 0.9878 and 35.26 and segmentation accuracy as 98.93%. The performance measure for classification are considered as sensitivity, specificity, classification accuracy and achieved as 98.78%, 99.23%, 99.24% and computational time and archives as 24.1128 seconds The performance comparison the results from the support vector machine and conventional ELM machine learning model with the suggested SCA-ELM models are presented to validate the uniqueness of the research.

Keywords*: Histogram oriented Graph, Sine Cosine Algorithm, Fast and robust Fuzzy Local Information C Means, support vector machine,* Extreme Learning Machine.

CHAPTER-1

INTRODUCTION

1.1. Background of the study

The lungs are affected by COVID-19 viruses flooding our airways with debris and fluids. The human lungs are sensitive body organ which is affected by COVID-19 quickly. In covid attacks the epithelial cells lining (American Lung Association, 2021). Early detection and diagnosis are a critical factor to control the COVID-19 spreading before seriously affecting lung. The patients affected by lungs disease are taken to hospitals and the process of X-Ray has been adopted to lungs to identify related virus, but it is difficult for the doctors to get information from the images of lungs. Nowadays, artificial intelligence playing a vital role in detecting diseases efficiently and effectively. The common features sharp costophrenic angles, and demarcated hemi diaphragms, sharp borders of heart are the components of Chest X-ray of normal patients (Lu S., et al., 2018). The medical imaging gains its importance to segment and classify the diseases from the images through different segmentation and classification techniques.

The classification of diseased and non-diseased category from chest x-ray images is also important for medical practitioners and radiologists. Efficient CovidNet proposed (Pedro S., et al.', 2020) along with a voting-based approach and a cross-dataset analysis with accuracy of 87.6%. A deep learning-based approach (Athanasios et al. 2020) has been proposed for the boundaries detection in images where COVID symptoms manifestation becomes apparent. An automatic detection system of COVID-19 (Xiang et al., 2020) by utilizing GoogLeNet-COD.

A convolutional neural network containing seven layer was proposed in (Yu-Dong et al., 2018) to have data augmentation and stochastic pooling methods. The size of the dataset, which would significantly affect the performance of networks, is still quite limited. In (Shui-Hua et al., 2020) lung diseases classification pipeline based on transfer and InceptionV3 deep model classifier is presented. Deep neural network (DNN) method (Shayan et al., 2020) proposed based on the fractal feature of input images achieves an accuracy of 93.2% and sensitivity 96.1%) a seven-layer standard convolutional neural (Yu-Dong et al., 2018), ResNet (Uboho et al., 2020) performed the experiments of training, an improved convolutional neural network (ICNN,)[15] etc for classification from chest x-ray images. Computer vision-based diagnosis with BBO algorithm

(Shui-Hua et al., 2020) and get a better global optimal solution. Further to reduce noise from the images, the image enhancement technique is also proposed by utilizing the SCA algorithm. (Seyedali M. et al., 2016) proposed SCA algorithm, for search proxies in the SCA algorithm.

Normal patient's Chest X-ray clearly shows sharp costophrenic angles, and demarcated hemidiaphragms with sharp borders (Salehi S. et al, 2020). Fig. 1.1 shows the general chest region of humans from normal chest X-ray images.

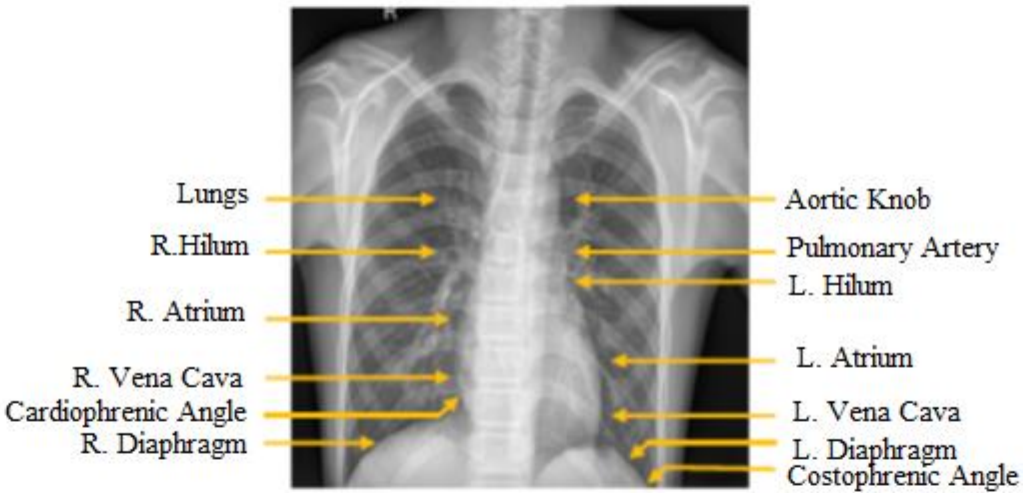

Fig. 1.1 X-ray of normal anatomy (Athanasios et al. 2020)

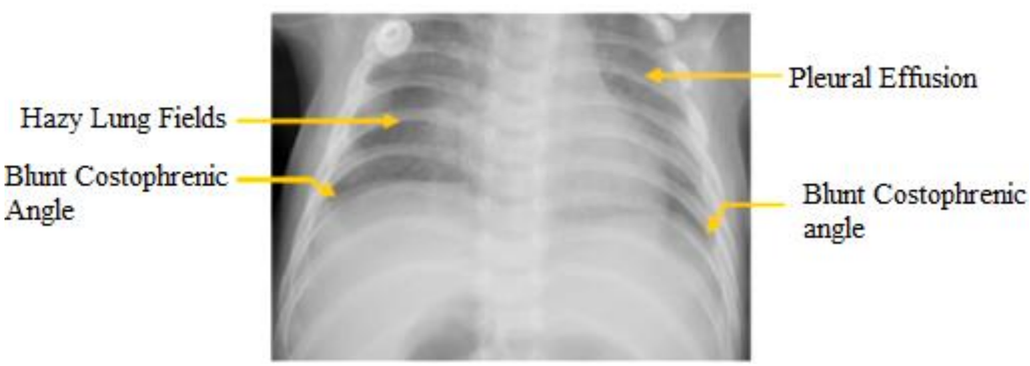

Fig. 1.2 Some symptoms of Covid-19 in PA chest X-ray (Athanasios et al. 2020)

The recent mentioned research works were not applied for lungs diseases related to covid, hence, motivated by this, a novel fast and robust FLICM (Fuzzy Local Information C-Means algorithm) segmentation technique and a HOG (Histogram of Oriented Gradients) feature based modified SCA-ELM model are proposed classification. Further to reduce noise from the images, the image enhancement technique is also proposed by utilizing the modified SCA algorithm.

1.2. Statement of the Problem

The diagnosis of COVID-19 at early stage is vital for lung disease treatment and becomes complex and arduous task. Suspected patients with respiratory problem or pneumonia are taken care by the hospital under consideration of emergency diagnostic measures with laboratory facilities for detecting the virus. The different tests such as blood gas analysis tests, blood count (CBC), and pleural effusion, samples are collected from the patients in the lab, which proceeds up valuable time. On the other side, the non-laboratory tests are the computer related techniques to detect the lungs affected regions by utilizing digital chest radiography (or X-ray) or CT scan. The X-Ray images are the good input for the purpose of classification and detection of virus tissues. At the same time we need to have automated detection system, for which we proposed a novel segmentation and classification techniques to solve the diagnosis issues.

1.3. Objective

1.3.1. General objective

The objective of the research work is to detect lung diseases related to covid-19 from x-ray images using proposed FRFLICM (Fast and Robust Fuzzy Local Information C-Means algorithm) segmentation method and classification through HOG (Histogram Oriented Graph) feature based SCA-ELM model.

1.3.2. Specific objective

- Enhancing image using Modified Sine Cosine Algorithm (MSCA) technique for preprocessing phase.
- Applying a FRFLICM (Fast and Robust Fuzzy Local Information C-Means algorithm) segmentation to remove noise and detect lung diseases from X-ray Images.
- Classify covid-19 related and other lung diseases though HOG feature and proposed sine cosine algorithm based extreme learning machine model.
- Investigating the application of the SCA optimization of weights of ELM model in classifying the useful information from lung x-ray image.

1.4. Significance of the Study

The growing incidences of lung diseases obstruct patients from receiving the authentic accommodation. In this regard, automating lung diseases detection could distribute many potential welfares. In a screening setting, it sanctions the inspection of a sizably voluminous number of images in less time than present observer determined methods which are subjective. It can additionally be a consequential diagnostic avail and can truncate the workload of trained graders, thereby truncating costs inside clinics.so that this study provides avail to radiologist, practitioner and surgeons in diagnoses of disease in very short time and with the high precision.

1.5. Scope and Limitations of the Study

The methodology has been developed for detection and relegation of lung diseases cognate to cov-19 will be tested X-ray images acquired from research image databases and some low-resolution images snapped from publications were withal considered (to test the robustness at low resolution and contrast). The genuine clinical validation of the work is withal beyond the scope of the current study and algorithm will not be implemented clinically which limits the testing step only to the images from the database and the snapped images. Additionally, the methodology developed will be implemented entirely on only a MATLAB platform.

1.6. Contribution of the Research Work

The research work emphases on three contributions based on image enhancement, image segmentation and classification. The contributions are summarized as follows:

- In the first aspect, we are proposing an image enhancement technique by modifying the parameters of the Sine Cosine Algorithm. The parameters such as position and velocity equations in the SCA algorithm has been modified to have better visualization and enhanced resolution of the images for this research purpose.
- In second aspect, an improvement to the fuzzy factor of FLICM based segmentation has been prepared to enhance the disease detection capability. Further, the improvement of fuzzy factor enhances noise reduction capability during segmentation. The mathematical analysis for the new FRFLICM segmentation has been derived to enhance the segmentation accuracy.

- In the third aspect, the modified sine cosine algorithm is proposed to update the weights of the ELM (Extreme Learning Model) model to enhance the classification performance of the classifier modified SCA-ELM classifier.

1.7. Thesis Organization

The thesis outline presented as follows:

Chapter-1 presents the review of mathematical analysis of FCM based segmentation algorithms, and classification models utilised for Lungs images related to COVID-19.

Chapter-2 presents literature assessment on image segmentation and classification followed by objective of study and thesis organization.

Chapter-3 presents the methodology of research which contains the research flow implementation, proposed modified SCA optimization algorithm for image enhancement, FRFLICM image segmentation and modified SCA–ELM deep learning model for the classification

Chapter -4 presents the results of image enhancement fitness, image segmentation, HOG feature descriptor and classification results comparison with the proposed modified SCA-ELM algorithm. Also presents the results discussion of the image enhancement, image segmentation and classification.

Chapter-5 presents thesis conclusion, future scope followed by reference.

CHAPTER-2

LITERATURE REVIEW

2.1 Related Works

As machine learning and deep learning are efficaciously applied in many fields, it has newly entered also the domain of health sectors. Recently, several researchers have studied different lung diseases and covid-19 identification and classification based on deep learning and machine learning approaches. The classifier extreme learning machine (Harmon et al., 2020) institutes a recent, modern method for image processing and data analysis, with promising results and large potential. The classifiers recycled to train the features are also not much operative. So, in this research brings in a new method of detecting and classifying the lung diseases by HOG Histogram of Oriented Gradients feature based modified SCA–ELM model. The study contracts with the extraction of features from the segmented area to detect and classify covid-19 and other lung diseases of medical lung X-ray images for a huge database. My result prompts end that with this proposed strategy it makes clinical specialists simple to take a choice in regard to analysis.

The FCM (Fuzzy C Means) (Ding Y et al., 2016) based segmentation techniques were failed to improve the noise reduction capability. To improve the noise reduction capability the FCM segmentations are improved with fuzzy factor with replacement of adjustable parameter α from the EnFCM (Ahmed M.N et al., 2020) segmentation. The fuzzy local information c-means clustering algorithm (FLICM) (Krinidis et al., 2010), segmentation replaced the adjustable parameter α by a new fuzzy factor in the objective function preserve the detailed image and improves the noise reduction capability. The FLICM segmentation improves the segmentation capability, but fails to remove Gaussian noise beyond 30%. The adaptive FCM algorithm based on noise detection (NDFCM) (Chen S. et al., 2004), by considering the local variance to enhance the noise reduction capability. The recent mention research works were not proposed any fast and robust segmentation technique for chest x-ray lungs images for improvement of noise reduction, so motivated by this, a novel fast and robust FLICM (Fuzzy Local Information C-Means algorithm) segmentation technique is proposed for image segmentation.

Further, extreme learning machine establishes a new, contemporary technique for image processing and data analysis. As machine learning and deep learning has been successfully applied in various domains, it has recently entered also the domain of health sectors. A computer vision-based diagnosis method based on WRE and SBBO is implemented (Shui-Hua W. et al., 2020) for detection. The technique comprises of three parts: WRE as feature extractor, FNN as classifier, and 3SBBO algorithm as optimizer. The disadvantages of this proposed smart COVID-19 diagnosis system are two-folds: Firstly, the wavelet Renyi entropy was extracted, Secondly, BBO was improved to speed up the convergence speed of BBO algorithm and get a better global optimal solution. U-Net structure (Athanasios et al., 2021) presented for segmenting COVID-19 infectious regions. The U-Net structure, re-configure the network parameters for detecting and segmenting infectious COVID-19 regions.

Recently, several researchers have studied different lung diseases and covid -19 identification and classification based on deep learning and machine learning approaches. The classifiers used to train the features are also not much effective. So, in this research brings in a new method of detecting and classifying the lung diseases by HOG feature based modified SCA –ELM model. The study agreements with the removal of features from the segmented area to detect and classify covid-19 and other lung diseases of medical lung X-ray images for a huge database.

2.2 Review of FCM Based Segmentation Technique

2.2.1 Fuzzy C Means Algorithms

Let $X = \{x_1, x_2, x_3 \ldots\ldots x_N\}$ are the data inputs. "FCM" (Ding Y. et al., 2016) is a method of clustering having objective function as

$$J_m = \sum_{k=1}^{N} \sum_{i=1}^{C} u_{ik}^m \|x_k - v_i\|^2 \tag{2.1}$$

Where m = 2, fuzziness coefficient, x_k is the i_{th} of n-dimensional measured data, v_i is centre of the cluster. The parameter 'm' is the fuzziness of partition and $\sum_{i=1}^{c} u_{ik} = 1$.

By using Lagrange method, we have

$$u_{ik} = \sum_{k=1}^{C} \left[\frac{\|x_k - v_i\|}{\|x_k - v_k\|} \right]^{-2/m-1}$$

$$\boldsymbol{v}_i = \frac{\sum_{k=1}^{N} \boldsymbol{u}_{ik}^m . x_i}{\sum_{k=1}^{N} u_{ik}^m} \tag{2.2}$$

The performance of FCM is not acceptable in noise reduction capability.

2.2.2 FCM_S: FuzzyClustering with Spatial Constraints and its Variants

(Ahmed et al. 2002) modified the quality FCM, in that the neighbourhood effect so as to regularize and the FCM_S is defined by modifying objective function as

$$J_m = \sum_{i=1}^{c}\sum_{k=1}^{N} u_{ik}^{m}\|x_k - v_i\|^2 + \frac{\alpha}{N_R}\sum_{i=1}^{c}\sum_{k=1}^{N} u_{ik}^{m}\sum_{r\in N_k}\|x_r - v_i\|^2 \tag{2.3}$$

Where N_R is its "cardinality", x_r constitute the neighbour of x_k and N_k stands for the place of neighbours declining into a "window" around and $\sum_{i=1}^{c} u_{ik} = 1$. There are two necessary conditions for J_m is expressed as

$$u_{ik} = \frac{\left(\|x_k - v_i\|^2 + \frac{\alpha}{N_R}\sum_{r\in N_k}\|x_k - v_i\|^2\right)^{-\frac{1}{m-1}}}{\sum_{i=1}^{c}\left(\|x_k - v_i\|^2 + \frac{\alpha}{N_R}\sum_{r\in N_k}\|x_k - v_i\|^2\right)^{-\frac{1}{m-1}}} \tag{2.4}$$

$$v_i = \frac{\sum_{k=1}^{N} u_{ik}^{m}\left(x_k + \frac{\alpha}{N_R}\sum_{r\in N_k} x_r\right)}{(1+\alpha)\sum_{k=1}^{N} u_{ik}^{m}} \tag{2.5}$$

The second word $\sum_{r\in N_k} x_r \Big/ N_R$ in the numerator of (2.5) shows neighbour common gray value approximately. In order to decrease the computational complexity, (Chen and Zhang et al., 2004) cut down the region of "FCM_S" and the low-composite objective function written as follows:

$$J_m = \sum_{i=1}^{c}\sum_{k\in N_k} u_{ik}^{m}\|x_k - v_i\|^2 + \alpha\sum_{i=1}^{c}\sum_{k=1}^{N} u_{ik}^{m}\sum_{k\in N_k}\left\|\overline{x_k} - v_i\right\|^2 \tag{2.6}$$

Where $\overline{x_k}$ is a means of neighbouring pixels deceitful within a window around x_k .Further u_{ik} and v_i can also in FCM_S be extracting, as:

$$u_{ik} = \frac{\left(\left\|x_k - v_i\right\|^2 + \alpha\left\|\overline{x_k} - v_i\right\|^2\right)^{-\frac{1}{m-1}}}{\sum_{i=1}^{c}\left(\left\|x_k - v_i\right\|^2 + \alpha\left\|\overline{x_k} - v_i\right\|^2\right)^{-\frac{1}{m-1}}} \tag{2.7}$$

$$v_i = \frac{\sum_{k=1}^{N} u_{ik}^m \left(x_k + \alpha \overline{x_k}\right)}{(1+\alpha)\sum_{k=1}^{N} u_{ik}^m} \tag{2.8}$$

2.2.3 FCM Based on Kernel-Induced Distance (KFCM)

If $x = [x_1, x_2]^T$ and $\Phi(x) = \left[x_1^2, \sqrt{2}x_1x_2, x_2^2\right]^{\boldsymbol{T}}$, where x_i is the i[th] component of u. Then the distinctive radial basis function (RBF) and polynomial kernel is given by:

$$\boldsymbol{K}(u, y) = exp\left(\frac{-(\sum_{i=1}^{d} |x_i - y_i|^a)^b}{\sigma^2}\right) \tag{2.9}$$

The dimension of vector x is given by d, a≥ 0; 1$\leq b \leq 2$. and (X, X) =1” for all X. With the above alignment, the kernelized description of FCM [26] algorithm with the mapping Φ is given by:

$$J_m^\Phi = \sum_{i=1}^{c} \sum_{k=1}^{N} \boldsymbol{u}_{ik}^m \, \|\Phi(X_k) - \Phi(V_i)||^2 \tag{2.10}$$

Now through the kernel substitution, we have

$$\begin{aligned} \|\Phi(X_k) - \Phi(V_i)||^2 &= (\Phi(X_k) - \Phi(V_i))^T\left(\Phi(X_k) - \Phi(V_i)\right) \\ &= \Phi(X_k)^T\Phi(X_k) - \Phi(V_i)^T\Phi(X_k) - \Phi(X_k)^T\Phi(V_i) + \Phi(V_i)^T\Phi(V_i) \\ &= \boldsymbol{K}(X_k, X_k)\boldsymbol{K}(V_i, V_i) - 2\boldsymbol{K}(X_k, V_i) \end{aligned} \tag{2.11}$$

Specifically, if the kernel function $\boldsymbol{K}(u, y)$ is in use as the RBF (Radial Basis Function), Furthermore, for the purpose of convenience of handling, considering $a = 2$ and $b = 1$ in (2.9) for Gaussian RBF (GRBF) kernel, then, (2.10) can be rewritten as:

$$J_m^\Phi = 2\sum_{i=1}^{c}\sum_{k=1}^{N} \boldsymbol{u}_{ik}^m \left(1 - \boldsymbol{K}(X_k, V_i)\right) \tag{2.12}$$

Additionally, when the parameter σ in (2.9) is positive constant, the FCM and its robust version like the L_p norm-based clustering algorithms as from (2.9) we have,

$$\boldsymbol{K}(x,y) \approx 1 - [(-(\sum_{i=1}^{d} |x_i - y_i|^{a})^{b})/(\sigma^2)]$$

Thus, $J_m^{\Phi} = (2/\sigma^2)\sum_{i=1}^{c}\sum_{k=1}^{N}\boldsymbol{u}_{ik}^{m}\,(\sum_{j=1}^{d}|x_{kj} - v_{ij}|^{a})^{b}$

Obviously, if $a = p$ and $b = (1/p)$, J_m^{Φ} reduces the objective function based on the L_p standard.

By an optimization technique for J_m^{Φ} to be at local minimum can be written as

$$\boldsymbol{u}_{ik} = \frac{(1-\boldsymbol{K}(X_k,V_i))^{-\frac{1}{(m-1)}}}{\sum_{j=1}^{c}(1-\boldsymbol{K}(X_k,X_j))^{-\frac{1}{(m-1)}}} \tag{2.13}$$

$$\boldsymbol{v}_i = \frac{\sum_{k=1}^{n}\boldsymbol{u}_{ik}^{m}K(X_k,V_i)X_k}{\sum_{k=1}^{n}\boldsymbol{u}_{ik}^{m}K(X_k,V_i)} \tag{2.14}$$

2.2.4 KFCM_S: FCM with Spatial Constraints Based on Kernel-Induced Distance

The new objective function during the newly-convince distance measure substitution

$$JS_m^{\Phi} = \sum_{i=1}^{c}\sum_{k=1}^{N}\boldsymbol{u}_{ik}^{m}\left(1-\boldsymbol{K}(X_k,V_i)\right) + \frac{\alpha}{N_R}\sum_{i=1}^{c}\sum_{k=1}^{N}\boldsymbol{u}_{ik}^{m}\sum_{r\in N_k}(1-\boldsymbol{K}(X_k,V_i) \tag{2.15}$$

An iterative algorithm of (2.13) with respect to u_{ik} and v_i can also be derived as mentioned in (2.14).

$$\boldsymbol{u}_{ik} = \frac{(\left(1-\boldsymbol{K}(X_k,V_i)\right) + \frac{\alpha}{N_R}\sum_{r\in N_k}(1-\boldsymbol{K}(X_r,V_i))^{m})^{-\frac{1}{(m-1)}}}{\sum_{j=1}^{c}(\left(1-\boldsymbol{K}\left(X_k,V_j\right)\right) + \frac{\alpha}{N_r}\sum_{r\in N_k}(1-\boldsymbol{K}(X_r,V_j))^{m})^{-\frac{1}{(m-1)}}} \tag{2.16}$$

$$\boldsymbol{v}_i = \frac{\sum_{k=1}^{n}u_{ik}^{m}\,(\boldsymbol{K}(X_k,V_i)X_k) + \frac{\alpha}{N_R}\sum_{r\in N_k}\boldsymbol{K}(X_r,V_i)X_r)}{\sum_{k=1}^{n}\boldsymbol{u}_{ik}^{m}\,(K(X_k,V_i) + \frac{\alpha}{N_R}\sum_{r\in N_k}\boldsymbol{K}(X_r,V_i)} \tag{2.17}$$

$$\boldsymbol{v}_i = \frac{\sum_{k=1}^{n}\boldsymbol{u}_{ik}^{m}\,(\boldsymbol{K}(X_k,V_i) + \frac{\alpha}{N_R}\sum_{r\in N_k}\boldsymbol{K}(X_r,V_i)X_k}{\sum_{k=1}^{n}\boldsymbol{u}_{ik}^{m}\,(\boldsymbol{K}(X_k,V_i) + \frac{\alpha}{N_R}\sum_{r\in N_k}\boldsymbol{K}(X_k,V_i)} \tag{2.18}$$

Similarly, a kernelized modification to (2.19) is

$$JS_m^{\Phi} = \sum_{i=1}^{c}\sum_{k=1}^{N} \boldsymbol{u}_{ik}^{m} \left(1 - \boldsymbol{K}(X_k, V_i)\right) + \alpha \sum_{i=1}^{c}\sum_{k=1}^{N} \boldsymbol{u}_{ik}^{m} \left(1 - K(\overline{X_K}, V_i)\right) \tag{2.19}$$

The objective function in (2.19) is minimized as:

$$\mathbf{u}_{\mathrm{ik}} = \frac{\left(\left(1 - \mathbf{K}(\mathrm{X_k}, \mathrm{V_i})\right) + \alpha(1 - \mathbf{K}(\overline{\mathrm{X_K}}, \mathrm{V_i}))\right)^{-\frac{1}{(\mathrm{m}-1)}}}{\sum_{\mathrm{j}=1}^{\mathrm{c}}\left(\left(1 - \mathbf{K}(\mathrm{X_k}, \mathrm{V_j})\right) + \alpha(1 - \mathbf{K}(\overline{\mathrm{X_K}}, \mathrm{V_j}))\right)^{-\frac{1}{(\mathrm{m}-1)}}} \tag{2.20}$$

$$\boldsymbol{V}_i = \frac{\sum_{k=1}^{n} \boldsymbol{u}_{ik}^{m} \left(\boldsymbol{K}(X_k, V_i).X_k) + \alpha\boldsymbol{K}.(\overline{X_K}, V_i)\overline{X_K}\right)}{\sum_{k=1}^{n} \boldsymbol{u}_{ik}^{m} \left(\boldsymbol{K}(X_k, V_i) + \alpha\boldsymbol{K}.(\overline{X_K}, V_i)\right)} \tag{2.21}$$

2.2.5 Enhanced Fuzzy C Means Algorithm

The EnFCM algorithm achieved by adding up image ξin FCM_S (Chen and Zhan, 2004) as:

$$\xi_k = \frac{1}{\alpha}\left(x_k + \frac{\alpha}{N_R}\sum_{j \in N_k} x_j\right) \tag{2.22}$$

Where $\xi_k$indicate the "gray value" of the k[th] pixel of the picture ξ, x_j represents the adjacent of $x_k$and the fast segmentation process is achieved with the objective function as:

$$J_s = \sum_{i=1}^{c}\sum_{l=1}^{q} \gamma_l\, \boldsymbol{u}_{il}^{m} (\xi_l - v_i)^2 \tag{2.23}$$

Where v_i represents the example of the i[th] cluster, γ_l is the amount of the pixels carry the gray value equal to l, where l=1, q. obviously, we have

$$\sum_{i=1}^{q} \gamma_l = N \tag{2.24}$$

And below the constraint so as to $\sum_{i=1}^{c} u_{il} = 1$ for any l, minimize J_s, correspondingly J_s to be at its limited extreme as follows

$$\boldsymbol{u}_{il} = \frac{(\xi_l - v_i)^{-\frac{2}{m-1}}}{\sum_{j=1}^{c} (\xi_l - v_i)^{-\frac{2}{m-1}}} \tag{2.25}$$

$$v_i = \frac{\sum_{i=1}^{q} \gamma_l \boldsymbol{u}_{il}^m \xi_l}{\sum_{l=1}^{q} \gamma_l \boldsymbol{u}_{il}^m} \tag{2.26}$$

EnFCM depends on the culled "window" size, the factor α and the "filtering" system. The value of α has to be culled astronomically immense enough so that it can truncate noise and, culled minuscule enough so that segmented image does not misplace its sharpness.

2.3 Review on Machine Learning Classification Method

2.3.1 Radial Basis Function Neural Network

The RBFNN (Sun Y.F et al., 2005, Kumar P. et al., 2015) is a three layered feed-forward neural network which uses Gaussian functions, and improves stopping criterion, learning rate, number of epochs than the ANN..

The radial basis function architecture is given in Fig. 2.1.

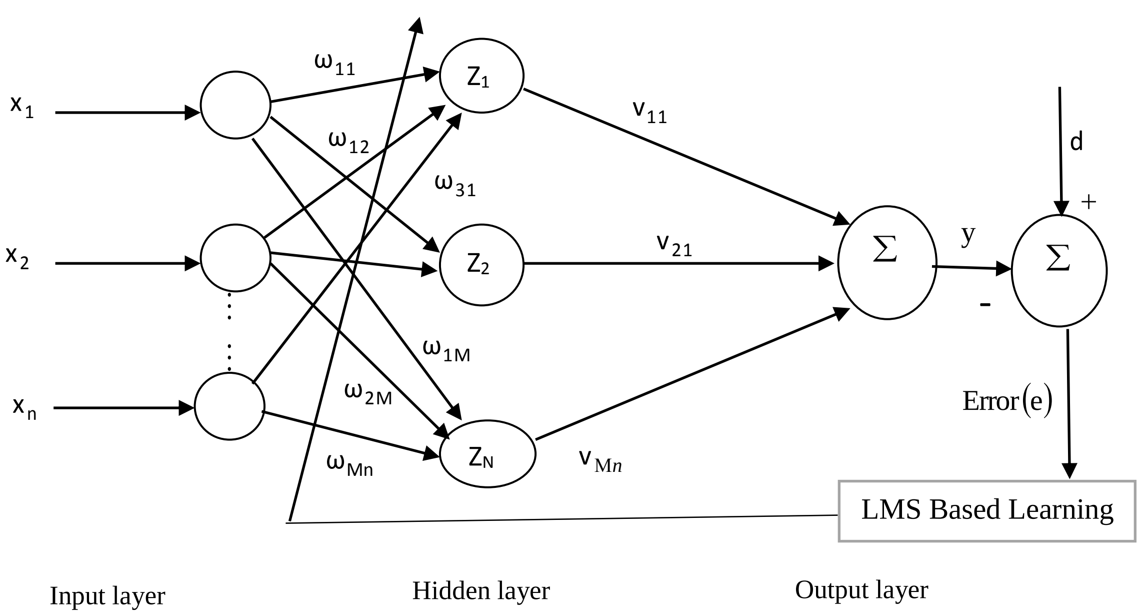

Fig. 2.1 LMS Based RBFN architecture

In this model, the activation function of the Nth hidden neuron is defined by a Gaussian Kernel as

$$Z_N(x) = e^{\left(\frac{-\|x_i - c_j\|^2}{2\sigma_n^2}\right)} \tag{2.27}$$

The output at the output layer is given by

$$y = \sum_{n=1}^{N} (v_{11}x_1 + v_{12}x_2 - - - - - - v_{Mn}x_n).e^{\left(\frac{-\|(x_N - C_M)\|^2}{2\sigma_M{}^2}\right)} \tag{2.28}$$

The error is calculated by subtracting the actual output from the desired output vector:

$$e = d_n - y_n \tag{2.29}$$

For n =1, 2, 3,……………..M

The Widrow Hoff's Least Mean Square algorithm:

$$w_{mn}(p+1) = w_{mn}(p) + \eta(p)x_{kn}^T e_{km} \tag{2.30}$$

for k = 1, 2, 3,…, K, n = 1, 2, 3,… m = 1, 2, 3,…,M

The mean square error is given by

$$MSE(e) = \frac{1}{N}\sum_{n=1}^{N}(d_n - y_n)^2 \tag{2.31}$$

Where "d" is the desired vector.

2.4 Support Vector Machine

The development of SVM made for the solution to an ANN (Mohd et al., 2011), (Rezaei et al., 2017), (Sonu et al., 2015) is universal and unique.

For binary classification in the diagram shows in Fig.2.2

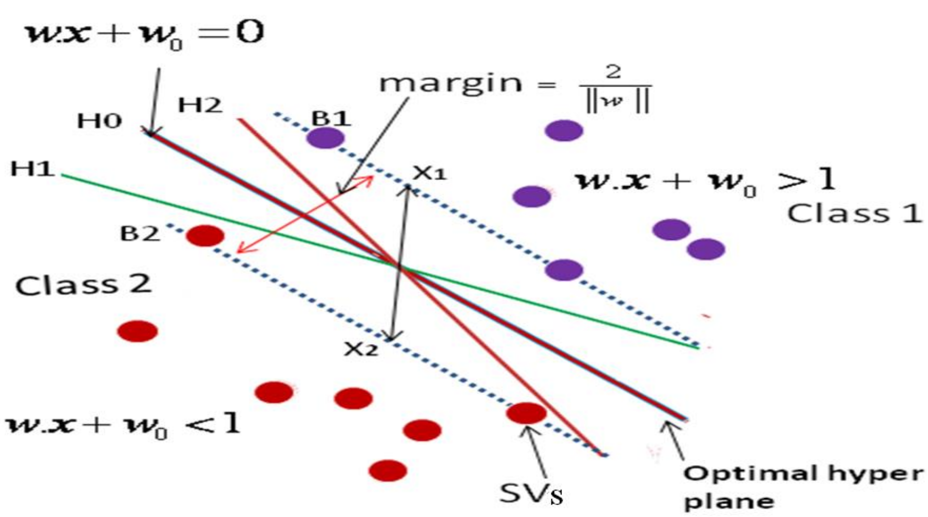

Fig .2.2 Two class problem with hyperplane analysis

The hyper planes H0, H1 and H2 achieve zero empirical risk, we have to maximize the margin which is same as minimizing the distance between the hyperplane and H0 generalizes optimally**.**

Thus by considering a decision function of the form

$f(x) = sgn(w.x + w_0)$ (2.32)

If $w.x + w_0 \rightarrow +ve \qquad f(x) = +1$

And $w.x + w_0 \rightarrow -ve \qquad f(x) = -1$ (2.33)

Considering two points (x_1, x_2) on the decision boundary B1 and B2, we can write

$w(x_1 - x_2) = 2.$

So the margin will be given by the projection of the vector $(x_1 - x_2)$ onto the normal vector to the hyperplane.

For the two classes of patterns, support planes, are given by,

$$\frac{|+1|}{\|w\|} + \frac{|-1|}{\|w\|} = \frac{|2|}{\|w\|} \qquad (2.34)$$

Where $\|w\|$ denotes the Euclidean norm of the weighting vector w

$$\text{Margin} = \frac{2}{\|w\|} \qquad (2.35)$$

Maximizing $\frac{2}{\|w\|}$ is same as minimizing $\|w\|$, so Maximizing the margin is thus equivalent to minimizing the function $\Phi(w) = \frac{1}{2}(w\,.\,w)$, subject to constraint $y_i[w.x_i + w_0] \geq 1.$

$$min \ \left\{\frac{1}{2}\|w\|^2 = \frac{1}{2}w.w\right\} \qquad (2.36)$$

$$w.r.t y_i(w.x_i + w_0) - 1 \geq 0$$

By introducing Lagrangian multipliers$(\alpha_1, \alpha_2, \ldots\ldots\ldots\ldots \alpha_N) \geq 0$, the equation (2.36) can be converted to the Lagrangian primal objective function

$$L(w, w_0, \alpha) = \frac{1}{2}(w^T.w) - \sum_{i=1}^{N} \alpha_i\,[y_i(w.x_i + w_0) - 1] \qquad (2.37)$$

Where $L(w, w_0, \alpha)$is the Lagrangian function.

The minimum with respect to w and w_0 of the Lagrangian, $L(w, w_0, \alpha)$, is given by,

$$\frac{\partial L}{\partial w_0} = 0 \Rightarrow \sum_{i=1}^{N} \alpha_i\, y_i = 0 \qquad (2.38)$$

and $$\frac{\partial L}{\partial w} = 0 \Rightarrow w = \sum_{i=1}^{N} \alpha_i\, y_i x_i \qquad (2.39)$$

The data points x_i for which $\alpha_i > 0$ are those points that are lie on the margins as well as inside the margin is called support vectors. From the solution given in equation (2.39), most of the α_i are zero.

Support vectors are the patterns which is most informative for the classification task. At the end of the training period, such a pattern will be one of the support vectors.

Solution for w can be written in a quadratic equation

$$W(\alpha) = \left\{\sum_{i=1}^{N} \alpha_i - \frac{1}{2}\sum_{i=1}^{N}\sum_{j=1}^{N} \alpha_i\alpha_j\, y_i y_j \langle x_i, x_j \rangle\right\} \tag{2.40}$$

Subject to $\sum_{i=1}^{N} \alpha_i\, y_i = 0$ where α_i is the hyper parameter or Lagrangian multiplier.

For non-separable data, we have

$$x_i * x_j = \Phi(x_i).\Phi(x_j) \tag{2.41}$$

The kernel function is given by

$$\Phi(x_i).\Phi(x_j) \to K(x_i, x_j) \tag{2.42}$$

Therefore the RBF kernel is given by

$$K(x_i, x_j) = e^{-\|x_i - x_j\|^2 / 2\sigma^2} \tag{2.43}$$

The point of estimates of the weights $W = \{w_j\}_{j=0}^{N}$ needed by SVM, such that the linear combination of the base functions $\Phi = \{K(x_i, x_j)\}_{i,j=1}^{N}$ fits the training targets closely. At the same time, it reduces the complexity of computation by forcing the majority of the weights to zero.

The SVM predictions is given by

$$y_i(x, w) = f_{svm}(x, w) = \sum_{i=1}^{N} w_i\, K(x, x_i) + w_0 \tag{2.44}$$

$$y(x, w) = \Phi(x)w \tag{2.45}$$

And $w = [w_0, w_1, w_2, \ldots\ldots w_N]^T$

Where $K(x, x_i)$ is a RBF kernel function and Φ is an augmented kernel matrix and is given by

$$\Phi = \begin{bmatrix} K(x_1, x_1) & K(x_1, x_2)\cdots & K(x_1, x_N) \\ K(x_2, x_1) & K(x_2, x_2)\cdots & K(x_1, x_1) \\ \vdots & \vdots\ddots & \vdots \\ K(x_N, x_1) & K(x_N, x_1)\cdots & K(x_N, x_N) \end{bmatrix}$$

For pattern classification problem, SVM we have to maximize

$$W(\alpha) = \sum_{i=1}^{N} \alpha_i - \frac{1}{2}\sum_{i=1}^{N}\sum_{j=1}^{N} \alpha_i y_i \alpha_j\, y_j K(x_i, x_j) \tag{2.46}$$

Subject to $\sum_{i=1}^{N} \alpha_i y_i = 0$ where α_i, α_j are the hyper parameters and $i = 1,2, \ldots\ldots\ldots N$

The decision function is given by

$$f(x) = sgn\left(\sum_{i=1}^{N} \alpha_i y_i K(x_i, x_j) + w_0\right) \quad (2.47)$$

Recently, several researchers have studied different lung diseases and covid -19 identification and classification based on deep learning and machine learning approaches. The classifiers used to train the features are also not much effective. So, in this research brings in a new method of detecting and classifying the lung diseases by HOG feature based SCA –ELM model. The study contracts with the withdrawal of features from the segmented area to detect and classify covid-19 and other lung diseases of medical lung X-ray images for a large database. The result prompts end that with this proposed strategy it makes clinical specialists simple to take a choice in regard to analysis.

2.5 Lungs image affected by Covid-19

The case studies of the COVID-19, we have identified the properties of the COVID-19 virus, associated disease symptoms taken from various sources, to classify the COVID-19 diseases for images. The COVID-19 dataset collected from Kaggle website. We emphasized the statistical significance of these measures for the purpose of detection and classification of COVID-19" diseases also. The Fig. 10 shows the chest X-Ray images from public hospitals of "São Paulo – Brazil" from March 15 to April 15, 2020

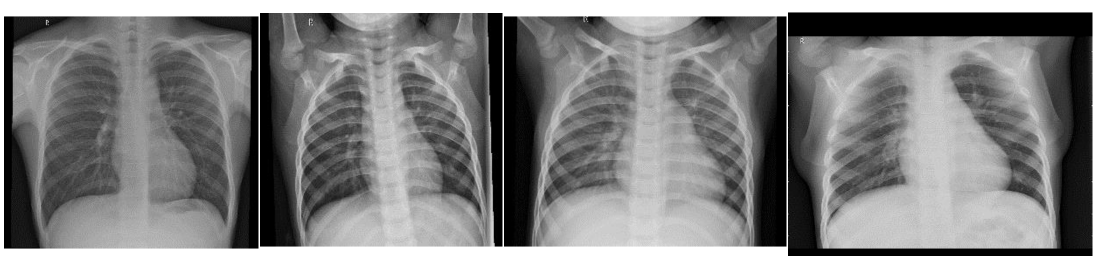

Fig.2.3 Normal covid-19 Chest images of four cases (Patients)

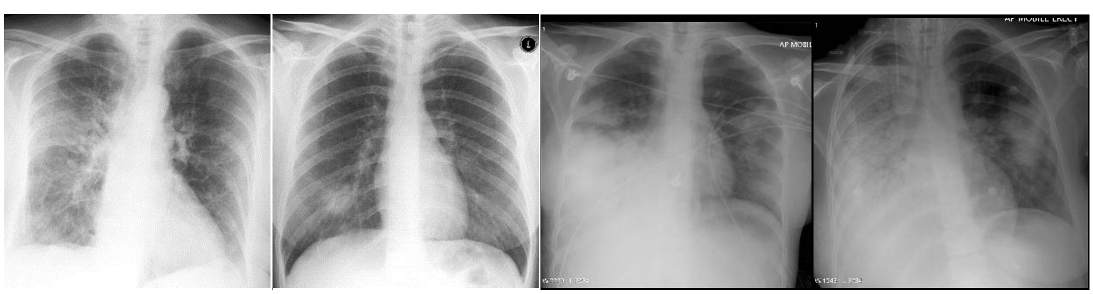

Fig.2.4 Pneumonia COVID-19 chest images of four cases (Patients)

Fig.2.5 MERIS images of chest and lungs

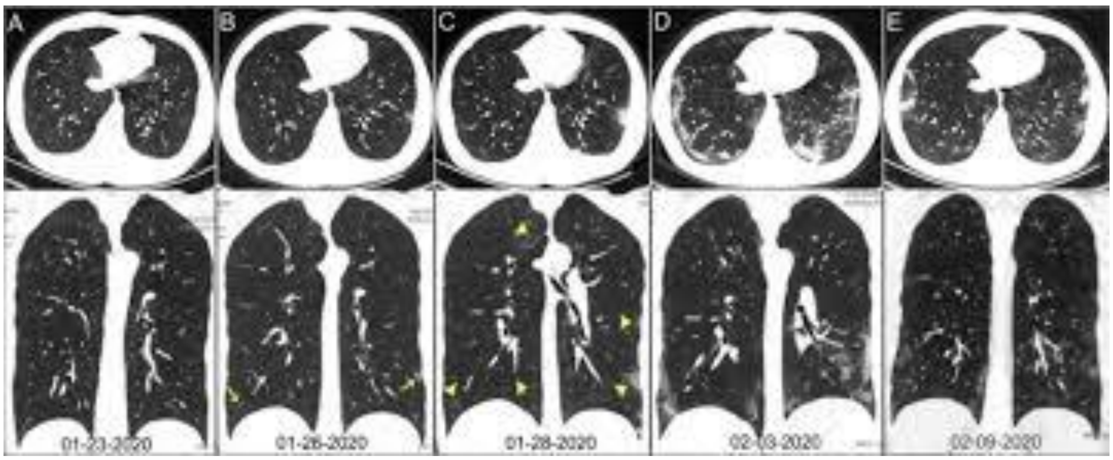

Fig.2.6 SARIS Images of chest and lungs

CHAPTER-3

METHODOLOGY

3.1 Research flow diagram

The research work followed the steps as: (i) The Lungs images collected and enhanced by modified SCA technique and segmented by the novel FRFLICM algorithm, Further (ii) the segmented images undergone HOG feature extraction (iii) In the third stage, the extracted features are fed as input to the proposed MSCA weight optimized ELM model for the classification of the Lungs diseases. (iv) In the fourth stage, the classification results comparison of the models are presented.

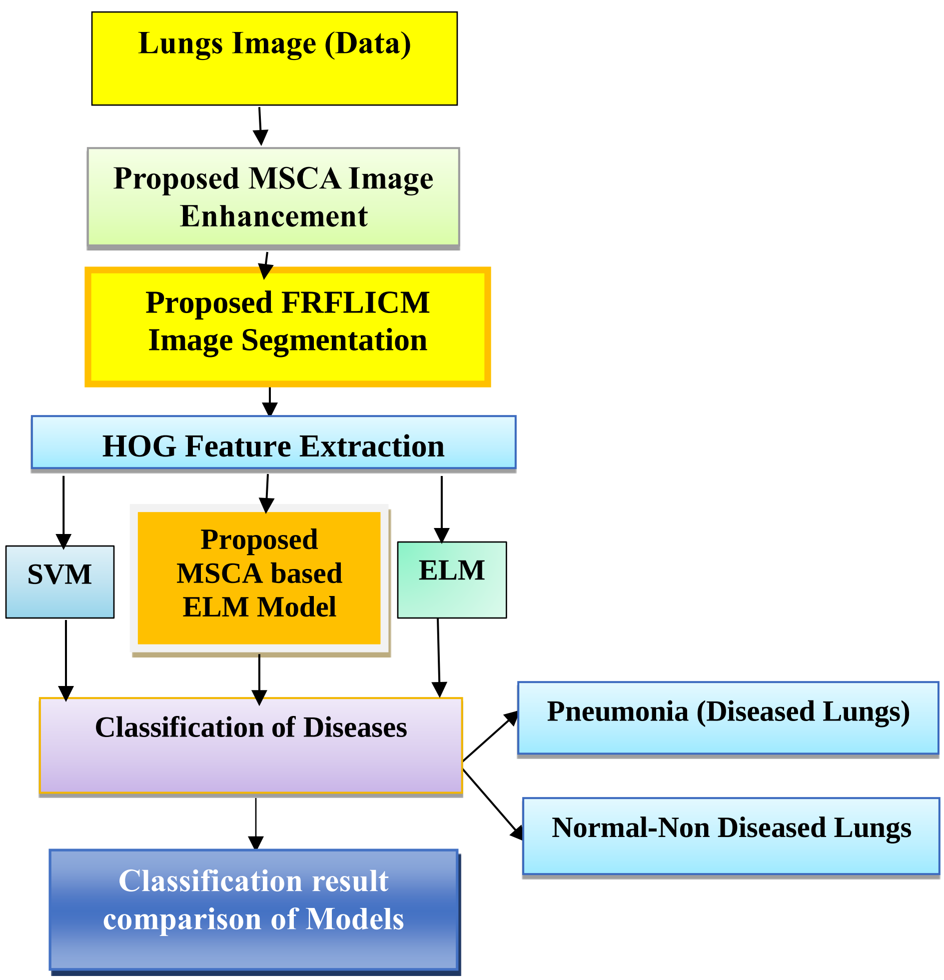

Fig. 3.1 Research flow diagram

3.2 Implementation

The research flow diagram indicates the step by step accomplishment of the research work. Further the block diagram shows the flow of algorithm application for detection and classification of lung disease related to Covid-19.

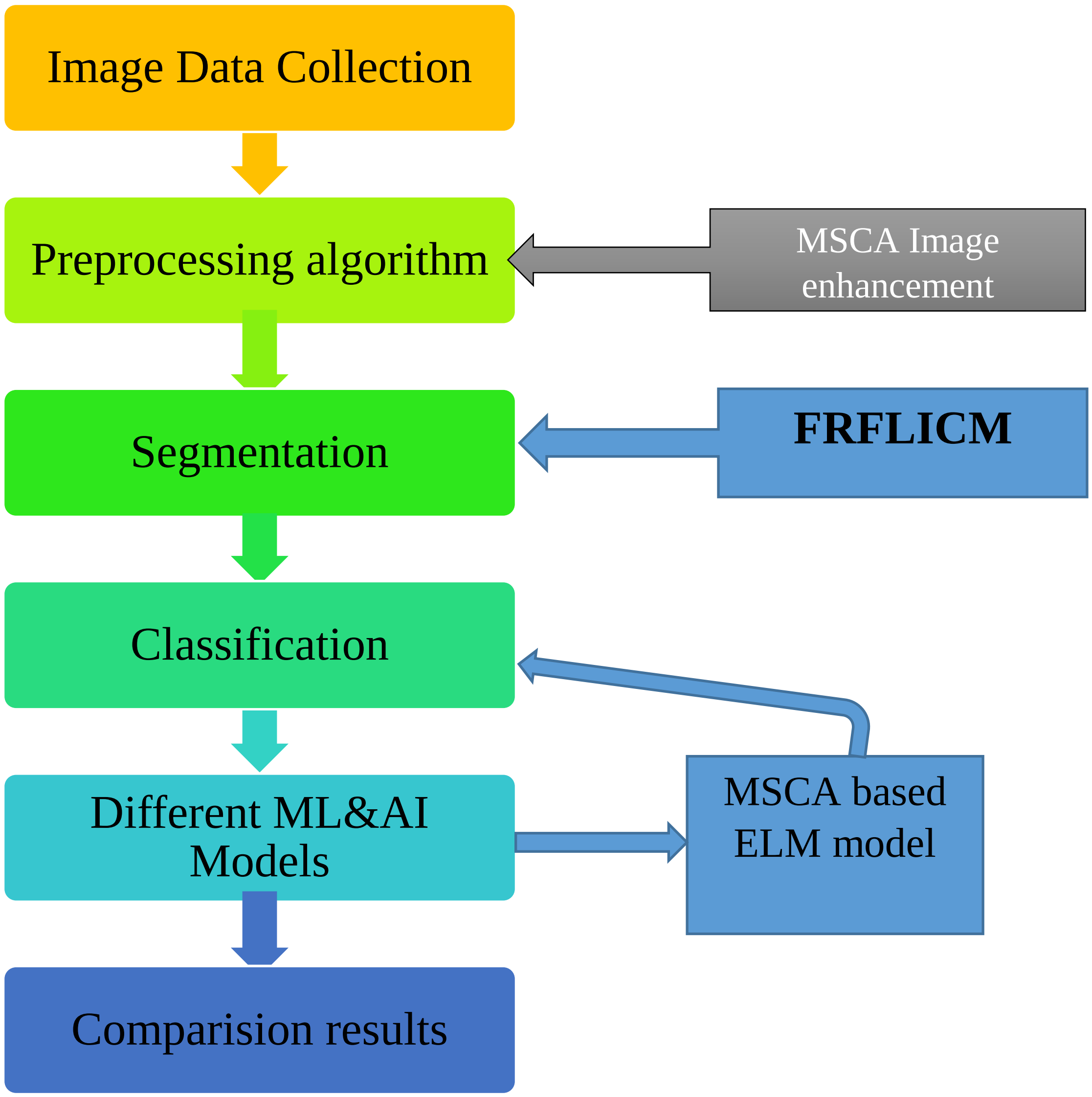

Fig. 3.2 Block Diagram Representation

3.3 Histogram of Oriented Gradients (HOG): Feature Extraction

The HOG descriptor is a geometric and photometric with Gradients (x and y directions) which are useful features that can signify complex shapes, such as edges and corners. The direction of the gradient represents the change of pixel intensity in an image. For an image $f(x, y)$, the gradient of the image can be represented as:

$$\nabla f = \begin{bmatrix} g_x \\ g_y \end{bmatrix} = \begin{bmatrix} \frac{\partial f}{\partial x} \\ \frac{\partial f}{\partial y} \end{bmatrix} \quad (3.1)$$

Here, $\frac{\partial f}{\partial x}$ is the derivative of the image with respect to x and $\frac{\partial f}{\partial y}$ is the derivative of the image with respect to y. Then we can derive as:

$$f_x(x) = \frac{\partial f}{\partial x} = f(x+1) - f(x-1) \quad (3.2)$$

$$f_y(y) = \frac{\partial f}{\partial y} = f(y+1) - f(y-1) \quad (3.3)$$

$$g = \sqrt{(g_x)^2 + (g_y)^2} \quad (3.4)$$

$$\theta = \tan^{-1}\left(\frac{g_x}{g_y}\right) \quad (3.5)$$

$$H_{l2} = |H| = \sqrt{{h_1}^2 + {h_2}^2 + {h_3}^2 + {h_4}^2 + .. + {h_n}^2} \quad (3.6)$$

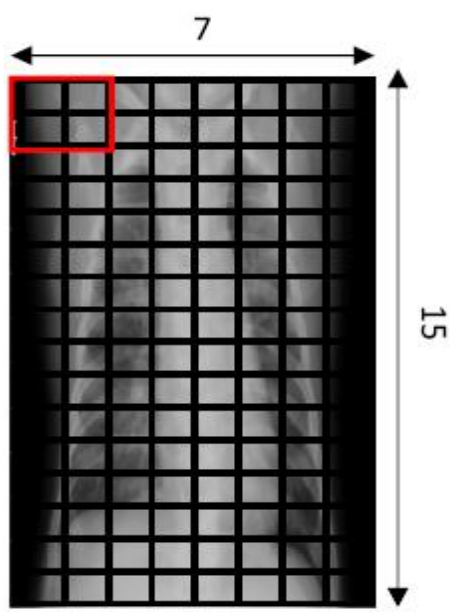

Fig. 3.3 HOG feature calculation

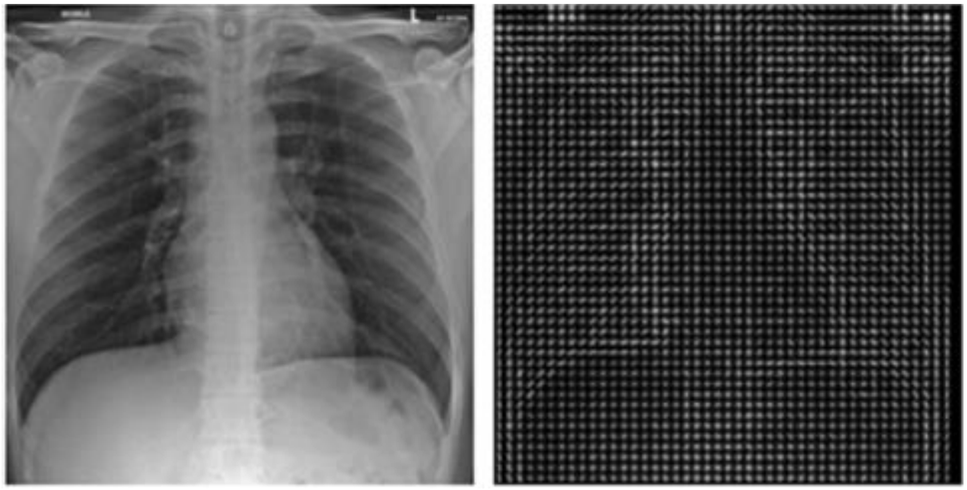

Fig. 3.4 Input image and its calculated histogram of oriented gradients

3.4 The Sine Cosine Algorithm (SCA)

Image enhancement is an important task before segmentation process. The contrast image enhancement has been utilized for brain tumors, and image enhancement by utilizing PSO and APSO algorithm proposed by swagat behera (swagat behera et al., 2015). But PSO (Particle Swarm Optimization), yet not applied for the for Lungs images previously. The Modified SCA algorithm is the novel image enhancement technique proposed in this research. The improvement in the learning parameters in SCA leads to a new velocity equation and "position equation". The mathematical analysis has been presented for the SCA to improve the performance of the optimization.

The sine cosine algorithm (SCA) (Seyedali M , 2016), (Ahmed et al., 2016) is a existed stochastic optimization algorithm which is based on the following update function for any search agent *Xi*:

According to sine cosine algorithm the position equation is updated as

$$X_i^{n+1} = \begin{cases} X_i^n + \alpha_1 \times sin(\alpha_2) \times \left|\alpha_3 p^{gbest} - X_i^n\right|, \alpha_4 < 0.5 \\ X_i^n + \alpha_1 \times cos(\alpha_2) \times \left|\alpha_3 p^{gbest} - X_i^n\right|, \alpha_4 \geq 0.5 \end{cases} \tag{3.7}$$

Where α_1,α_2, α_3, $\alpha_4$are the random variables and $\alpha_1$is given by

$$\alpha_1 = a\left(1 - \frac{n}{K}\right) \tag{3.8}$$

Where n is the current iteration, K is the maximum number of iterations.

The X_i^n signifies the "current position" and X_i^{n+1} signifies the "new position". At this point$|.|$ signifies the complete significance. The factor α_1 resolves the subsequently position areas of explore and discovers to investigate the gap to a superior amount. The factorα_2 signifies the direction of movement of on the way to or away from $x_i(n)$ .The parameter α_3 controls the present movement, throughout each iteration α_1,α_2, α_3 are simplified and the parameter α_4 uniformly switches among the sine and cosine functions.

The α_1 is the next position in the search, α_2 determines direction of movement, α_3 controls the current movement, and α_1 is given by

$$\alpha_1 = a\left(1 - \frac{n}{K}\right)$$

Where the current iteration is given by n , maximum numbers of iterations are denoted by K and a is a constant.

Fig. 3.5 shows that how the proposed equations define a space between two solutions in the search space.

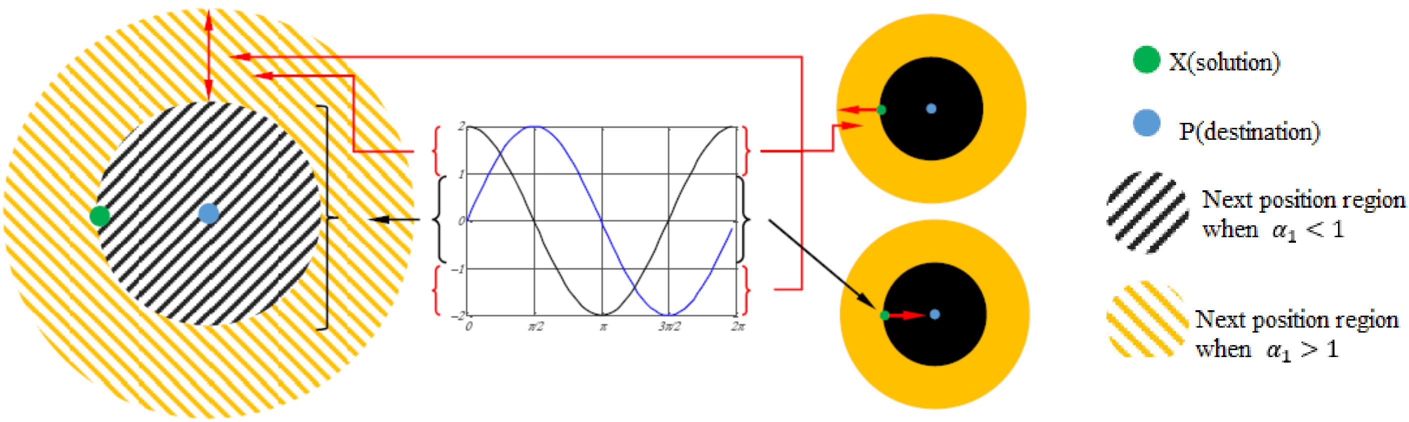

Fig: 3.5 Effects of Sine and Cosine with range in [-2, 2] on the next position

3.4.1 MSCA Optimization

For speedy convergence of the parameter α_1 is adapted as

$$\alpha_{11} = \frac{1}{1+sigmoid(\alpha_1)} \tag{3.9}$$

And the resultant position equation is specified with modification factorα_{11} is obtained as

$$X_{ij}^{n+1} = \begin{cases} X_{ij}^n + \alpha_{11} \times sin(\alpha_2) \times |\alpha_3 y_i^n - X_i^n|, \alpha_4 < 0.5 \\ X_{ij}^n + \alpha_{11} \times cos(\alpha_2) \times |\alpha_3 y_i^n - X_i^n|, \alpha_4 \geq 0.5 \end{cases} \tag{3.10}$$

Considering the image pixels movement according to position and velocity, the SCA algorithm is implemented as follows. The v_t and x_t are considered as velocity and position of the pixels in an image. According to the PSO [39] algorithm the velocity update equation is given by

$$v_t(n+1) = \kappa * v_t(n) + \beta_1 r_1\left(p_i^{best} - x_t(n)\right) + \beta_2 r_2\left(p^{gbest} - x_t(n)\right) \tag{3.11}$$

And the position update equation is given by

$$x_t(n+1)=x_t(n)+v_t(n+1) \tag{3.12}$$

Where κ is "inertia coefficient".

According to APSO [39], the velocity vector is presented to avoid mathematical complexity

$$v_t(n+1)=v_t(n)+\alpha \in_n +\beta\left[g^{best}-x_t(n)\right] \tag{3.13}$$

Where $\in_n$ is drawn from N(0,1).

In order to increase the convergence even further, we can also write the update of the location in a single step

$$x_t(t+1)=(1-\beta)x_t(t)+\beta g^{best}+\alpha \in_n \tag{3.14}$$

Now the position equation of SCA is updated with PSO as follows

$$\begin{aligned} X_i^{n+1} &= X_i^n+\alpha_1\times\sin(\alpha_2)\times\left|\alpha_3 p^{gbest}-X_i^n\right|+\beta_1 r_1\left(p_i^{best}-x_i(n)\right)+\beta_2 r_2\left(p^{gbest}-x_i(n)\right) \\ X_i^{n+1} &= X_i^n+\alpha_1\times\cos(\alpha_2)\times\left|\alpha_3 p^{gbest}-X_i^n\right|+\beta_1 r_1\left(p_i^{best}-x_i(n)\right)+\beta_2 r_2\left(p^{gbest}-x_i(n)\right) \\ V_i^{n+1} &= X_i^{n+1}+V_i^n \end{aligned} \tag{3.15}$$

Where α the learning parameter and the value is taken between [0.5, 1].

With the equations (3.13), (3.14), and (3.15) the PSO, APSO and modified SCA techniques are utilized for image enhancement and the corresponding results for fitness and entropy are presented in the section 4.

Table 3.1 Pseudo code: MSCA Algorithm implementation for Image enhancement

Pseudo code: SCA Algorithm implementation for Image enhancement
1. Initializing random position and velocity vectors.
2. Initialize the SCA parameters $\alpha_{11},\alpha_2,\alpha_3,\alpha_4$
3.Evaluate the evaluate fitness based on x_{ij}
4.%optimization loop
5.for i=1:k
6. for j=1:N
7. update(eqn(below) for sin)
$v_t(n+1)=v_t(n)+\alpha \in_n +\beta\left[g^{best}-x_t(n)\right]$
$x_t(t+1)=(1-\beta)x_t(t)+\beta g^{best}+\alpha \in_n$
8. update SCA parameter to obtain fitness

9. update the modified position and velocity equation

$$X_i^{n+1} = X_i^n + \alpha_1 \times \sin(\alpha_2) \times \left|\alpha_3 p^{gbest} - X_i^n\right| + \beta_1 r_1 \left(p_i^{best} - x_i(n)\right) + \beta_2 r_2 \left(p^{gbest} - x_i(n)\right)$$

$$X_i^{n+1} = X_i^n + \alpha_1 \times \cos(\alpha_2) \times \left|\alpha_3 p^{gbest} - X_i^n\right| + \beta_1 r_1 \left(p_i^{best} - x_i(n)\right) + \beta_2 r_2 \left(p^{gbest} - x_i(n)\right)$$

$$V_i^{n+1} = X_i^{n+1} + V_i^n$$

11. end for the loop j

12. end for the loop i

15.Stopping criteria: getting fitness as optimal solution

3.5 Fuzzy Local Information C-Means

(Cai et al., 2007) proposed the fast generalized FCM algorithm (FGFCM), but fails to improve the capability of noise reduction. However, EnFCM (Mishra S. et al., 2019) as well as FGFCM (Mishra S. et al., 2019), share a common crucial parameterα.

(Krinidis and Chatzi, 2010) proposed FLICM (Fuzzy Local Information C-Means), to improve the the noise reduction capability.

According to the FLICM (Krinidis and Chatzi, 2010), the fuzzy factor is given by:

$$G_{kv} = \sum_{\substack{k \in N_v \\ v \neq k}} \frac{1}{d_{vk} + 1} (1 - u_{kv})^m \|x_v - v_k\|^2$$

By using the definition of G_{kv}, the objective function of the fuzzy c means algorithm with local information is given by

$$J_s = \sum_{v=1}^{N} \sum_{k=1}^{c} u_{kv}^m \|x_v - v_k\|^2 + \sum_{v=1}^{N} \sum_{k=1}^{c} G_{kv} \tag{3.16}$$

Where the fuzzy factor is given by

$$G_{kv} = \sum_{\substack{k \in N_v \\ v \neq k}} \frac{1}{d_{vk}+1} (1 - u_{kv})^m \|x_v - v_k\|^2 \tag{3.17}$$

The fuzzy factorG_{kv}, improves noise reduction improves. The "fuzzy partition matrix" is given by

$$u_{kv} = \frac{1}{\sum_{j=1}^{c} \left(\frac{\|x_v - v_k\|^2 + G_{kv}}{\|x_v - v_j\|^2 + G_{jv}} \right)^{\frac{1}{m-1}}} \tag{3.18}$$

And

$$v_k = \frac{\sum_{k=1}^{N} u_{kv}^m x_v}{\sum_{v=1}^{N} u_{kv}} \tag{3.19}$$

Further the approaches described in the algorithms have generated effective clustering results for images, but contains some disadvantages:

3.5.1 Fast and Robust Fuzzy Local Information C Means (FRFLICM) Algorithm

To overcome the above mentioned disadvantages the fuzzy factor in objective function is modified to have some special characteristics:

Let the N sample data given by $X = \{x_1, x_2, x_3 \ldots\ldots x_N\}$. Fuzzy C Means [25] algorithm the cost function minimized as:

$$J_m = \sum_{k=1}^{N} \sum_{i=1}^{c} u_{ik}^m \tag{3.20}$$

Where v_i is the center of cluster (Ahmed et al, 2002) considered a parameter α and the objective function is given by

$$J_m = \sum_{i=1}^{c} \sum_{k=1}^{N} u_{ik}^m \|x_k - v_i\|^2 + \frac{\alpha}{N_R} \sum_{i=1}^{c} \sum_{k=1}^{N} u_{ik}^m \sum_{r \in N_k} \|x_r - v_i\|^2 \tag{3.21}$$

Where α controls the neighbors term. (Chen and Zhang, 2004) proposed a variant by taking mean to reduce the complexity, and the objective function is given by

$$J_m = \sum_{i=1}^{c} \sum_{k \in N_k} u_{ik}^m \|x_k - v_i\|^2 + \alpha \sum_{i=1}^{c} \sum_{k=1}^{N} u_{ik}^m \sum_{k \in N_k} \|\overline{x_k} - v_i\|^2 \tag{3.22}$$

Where $\overline{x_k}$ is a mean L.Szilágyi et al. [35] proposed enhanced fuzzy c means EnFCM algorithm where image ξ the original image and represented by

$$\xi_k = \frac{1}{\alpha}\left(x_k + \frac{\alpha}{N_k} \sum_{j \in N_k} x_j\right) \tag{3.23}$$

Where q represents the number of gray level and less than N, the gray value of k^{th}pixel of image ξ is given by ξ_k, $x_j$is neighbors of x_k, Now the new objective function is given by

$$J_s = \sum_{l=1}^{N} \sum_{k=1}^{c} \gamma_l\, u_{kv}^m \|\xi_l - v_k\|^2 \tag{3.24}$$

Where u_{il} represents the "fuzzy membership of gray" value l.

The FLICM (Krinidis et al., 2010) fuzzy factor is given by

$$G_{kv} = \sum_{\substack{k \in N_v \\ v \neq k}} \frac{1}{d_{vk}+1} (1 - u_{kv})^m \|x_v - v_k\|^2 \tag{3.25}$$

To increase the noise reduction competence the fuzzy factor is modified, and the new cost function is given by

$$J_s = \sum_{l=1}^{N} \sum_{k=1}^{c} \gamma_l \, u_{kv}^m \|\xi_l - v_k\|^2 + \sum_{v=1}^{N} \sum_{k=1}^{c} 1/\,exp\Big(\sum_{\substack{k \in N_v \\ v \neq k}} \frac{1}{d_{vk}+1} (1 - u_{kv})^m \|x_v - v_k\|^2 \Big) \tag{3.26}$$

With the new objective function, the segmentation accuracy has been improved and presented in the result section.

3.6 Extreme Learning Machine (ELM)

3.6.1 Motivation

The motivations is as follows

1. ELM is a feed forward network
2. ELM requires less number of neurons
3. ELM has higher classification capability

Extreme learning machine used to reduces the memory and computational time of classification (Deepa et al.,2013).

The ELM output with L hidden neurons is represented by

$$y = \sum_{k=0}^{L} \beta_k h_k(w_k; x)$$

where $h(w;x) = [1, h_1(w_1;x), \ldots\ldots, h_L(w_L;x)]$is the hidden layer, input $x = [x_1 \ldots\ldots x_N]$ and β is the weight vector of all hidden neurons to an output neuron to be logically analyzed. $h_k(\cdot)$ which is the activation function of hidden layer.

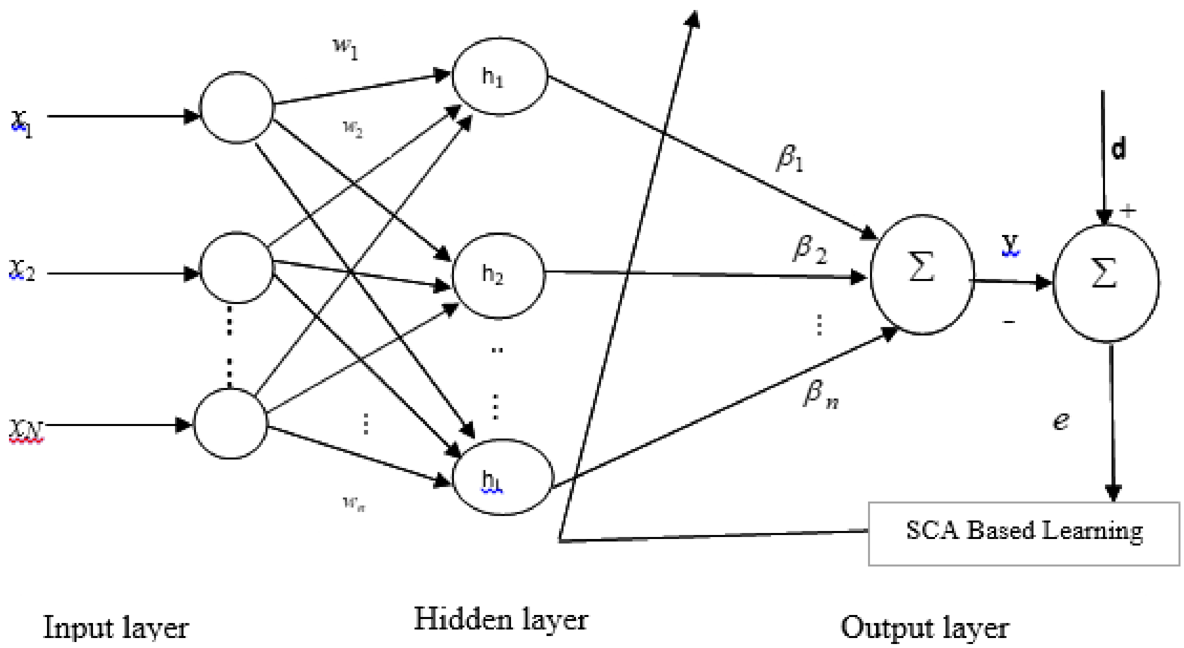

Fig: 3.6 SCA Based ELM architecture

3.6.2 ELM Model with MSCA optimization

This research proposes a modified SCA for ELM (Soria-Olivas et al., 2011), (Tipping et al., 2001), (Vong et al., 2013) weight optimization (called MSCA-ELM) that optimizes the output weights of ELM classifier, support vector machine (SVM) (Soria-Olivas et al., 2011), (Tipping et al., 2001), is considered for comparison with the proposed MSCA-ELM model.

The ELM model output is given by

$$y = \sum_{k=0}^{L} \beta_k h_k(w_k; x) \tag{3.27}$$

where $h(w;x) = [1, h_1(w_1;x), \ldots\ldots, h_L(w_L;x)]$ is the hidden matrix and input $x = [x_1 \ldots . x_N]$ and β is the weight vector. Equation (3.38) can be written as

$$H\beta = y \tag{3.28}$$

Where H is the $N \times (L+1)$ hidden layer feature-mapping matrix, whose elements are as follows:

$$\boldsymbol{H} = \begin{bmatrix} \mathbf{1} & \boldsymbol{h_1}(\boldsymbol{w_1}; \boldsymbol{x_1}) & \cdots & \boldsymbol{h_L}(\boldsymbol{w_N}; \boldsymbol{x_1}) \\ \vdots & \vdots & \vdots & \vdots \\ \mathbf{1} & \boldsymbol{h_1}(\boldsymbol{w_1}; \boldsymbol{x_N}) & \cdots & \boldsymbol{h_L}(\boldsymbol{w_N}; \boldsymbol{x_N}) \end{bmatrix} \tag{3.29}$$

And

$$h_L(w_N; x_N) = [w_1x_1 + w_1x_1 \ldots\ldots\ldots w_Nx_N].e^{\left(\frac{-\|(x_N - v_i)\|^2}{2\sigma_n{}^2}\right)}$$

Where σ_n^2 is the controlling parameter and $\|x_i - c_j\|$ is the "Euclidean distance"..

The i^{th} row of H is the hidden layer's output vector for an instance x. Equation (3.29) is a linear system, which is solved by

$$\beta = \boldsymbol{H}^{\dagger} d, \qquad \boldsymbol{H}^{\dagger} = (\boldsymbol{H}^{\boldsymbol{T}}\boldsymbol{H})^{-1}\boldsymbol{H}^{\boldsymbol{T}} \tag{3.30}$$

Where $H^{\dagger}$ is the Moore–Penrose generalized inverse of matrix H

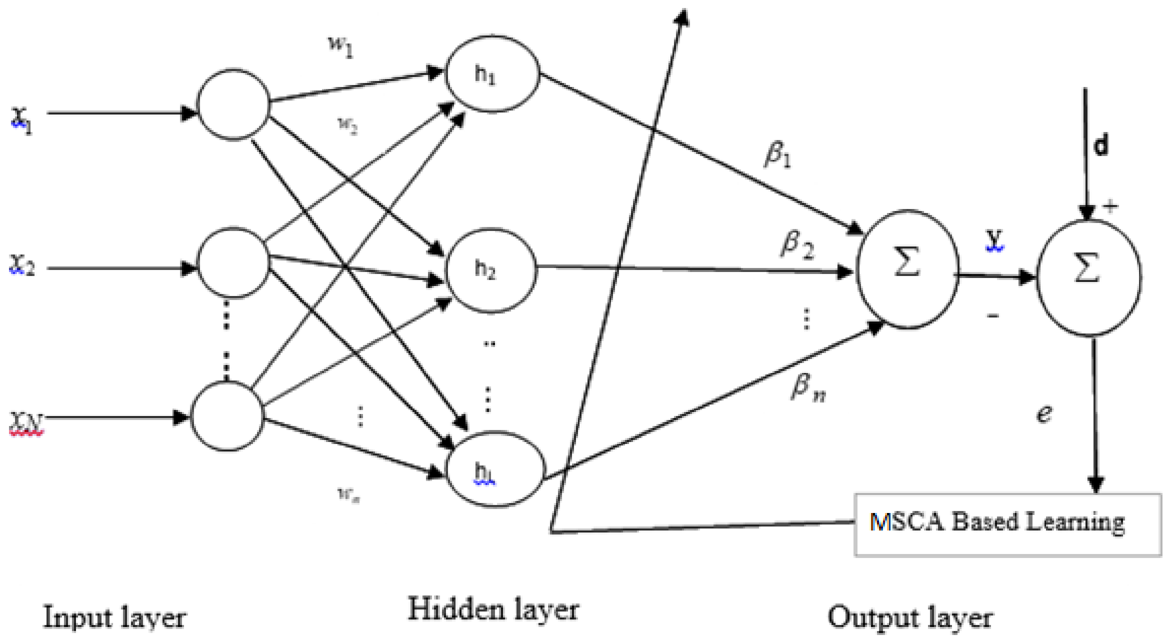

Fig.3.7 MSCA Based ELM model

And $d = \begin{bmatrix} d_1 \\ d_2 \\ \vdots \\ d_n \end{bmatrix}, \quad \beta = \begin{bmatrix} \beta_1 \\ \beta_1 \\ \vdots \\ \beta_n \end{bmatrix}$

3.6.3 Proposed learning algorithm steps:

The Algorithm has a training set $\aleph = \{(x_i, d_i) | x_i \in R^n, t_i \in R^m, i = 1, \ldots\ldots N\}$ activation function $h(x)$, 1: input weight w_i , $i = 1, \ldots, N$.,2: calculation of H.3: The output calculation of weight β is given by

$$\beta = \boldsymbol{H}^{+} d$$

Where $d = [d_1, \ldots\ldots, d_N]^T$

Table 3.2 Pseudo Code: MSCA weight optimization of Extreme Learning Machine

***PSEUDO CODE*:**

1. Initializing particles (ELM weights) with random position and velocity vectors.

2.Initialize the SCA position parameters α_1,α_2, α_3

%Starting of the loop
Initialize the weights W of the ELM to zero
Evaluate the objective function in the next phase to evaluate fitness at first step
4.%Program loop
for i=1:n

$$X_{ij}^{n+1} = \begin{cases} X_{ij}^n + \alpha_{11} \times sin(\alpha_2) \times |\alpha_3 y_i^n - X_i^n|, \alpha_4 < 0.5 \\ X_{ij}^n + \alpha_{11} \times cos(\alpha_2) \times |\alpha_3 y_i^n - X_i^n|, \alpha_4 \geq 0.5 \end{cases}$$

Update X_{ij}^{n+1} *for best fit*

%Update the weights by using the equation

For j=1:n

$$\hat{\beta}_j = \begin{cases} H^{.T} \left(\frac{1}{\lambda} + .HH^{.T} \right)^{-1} d_j \\ \left(\frac{1}{\lambda} + H.H^{.T} \right)^{-1} H^{.T} d_j \end{cases}$$

end for the loop j

end for the loop i

4. Continue till converges, else go to step 4, and repeat until convergence is satisfied.

3.7 Dataset Description

The real time data has been collected from Adama hospital and Kaggle Dataset to reach the specific objectives. The data contains real time lung diseases occurrence from the X-ray image.. A total of 500 images consisting of different lungs disease x-ray images are collected. The images are under gone image enhancement and segmentation and features are extracted. There are six features are extracted from the images , so a total of 500x6=3000 features are collected and the features are treated as dataset for the research. Out of 3000 data, 70% of the data are utilized for training and 30% of the data are utilized for testing and validation. Some of the images of the diffent lungs disease are presented in Fig.3.8 to Fig. 3.10.

Fig. 3.8 Lungs image affeected by Lungs cancer

Fig.3.9 Lungs image affeected by Lobar Pneumonia

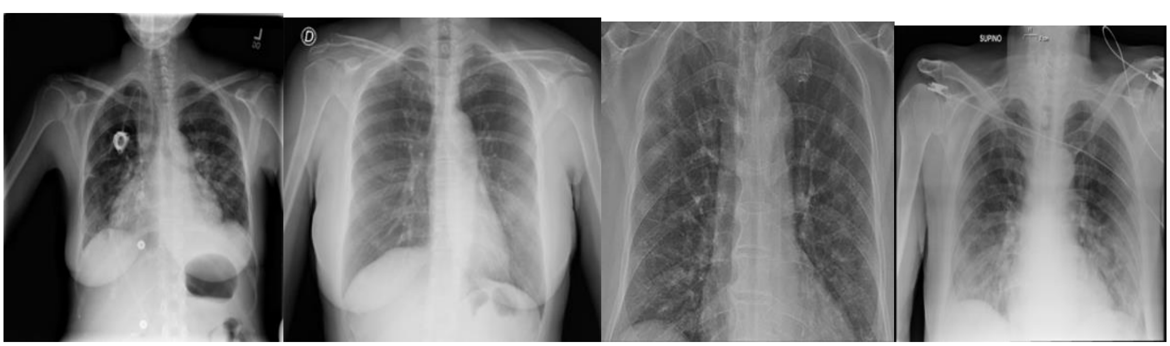

Fig.3.10 Lungs image affeected by Bacrriol Pneumonia

CHAPTER-4

SIMULATION RESULTS AND DISCUSSION

This thesis work has been carried out using MATLAB 2021a simulation sofware package. The simulation results are based on the previous chapters‘ mathematical concept and compared the image enhancement using MSCA algorithm with the existing SCA & PSO algorithm. In addition to enhancement, the lung diseased region oreintations of the different loacations are identified using HoG feature extractor. The enhanced images are segmented by using the proposed FRLICM and compared with the existing model FLICM and FGFCM segmentation techniques. Finally, the performance computional time is calculated for SVM, ELM, SCA-ELM and MSCA-ELM.

4.1 Image Enhancement Results

Image enhancement is the process of adjusting images to make more suitable for display or further analysis. In this section, the lower fitness value means better enhanced image. In fig. 4.1 to 4.11, the X axis of the graphes represents number of iteration and Y axis dtermines the fitness value of normal lung, pneumonia, tuberclosis and covid affected lungs using PSO, SCA and MSCA. In the graphes, the proposed MSCA was shown with lime color line and PSO & SCA were shown with blue & red color lines respeectively.

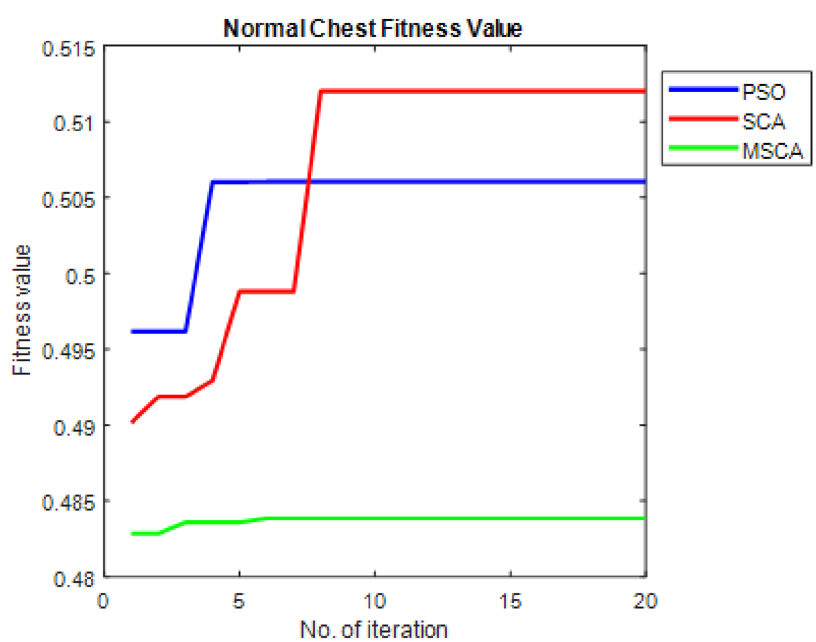

Fig.4.1 Normal Lungs image enhancement fitness Value by using PSO, SCA and MSCA

In fig. 4.1 shows the normal lungs image enhancement and it is observed that the fitness value is nearly 0.483 in the case of proposed MSCA optimization technique, which is less than in comparision to the PSO (0.507) and SCA (0.513) optimization technique. This indicate that the MSCA has bettter clarity of image enhacement than PSO & SCA in the case normal lung image.

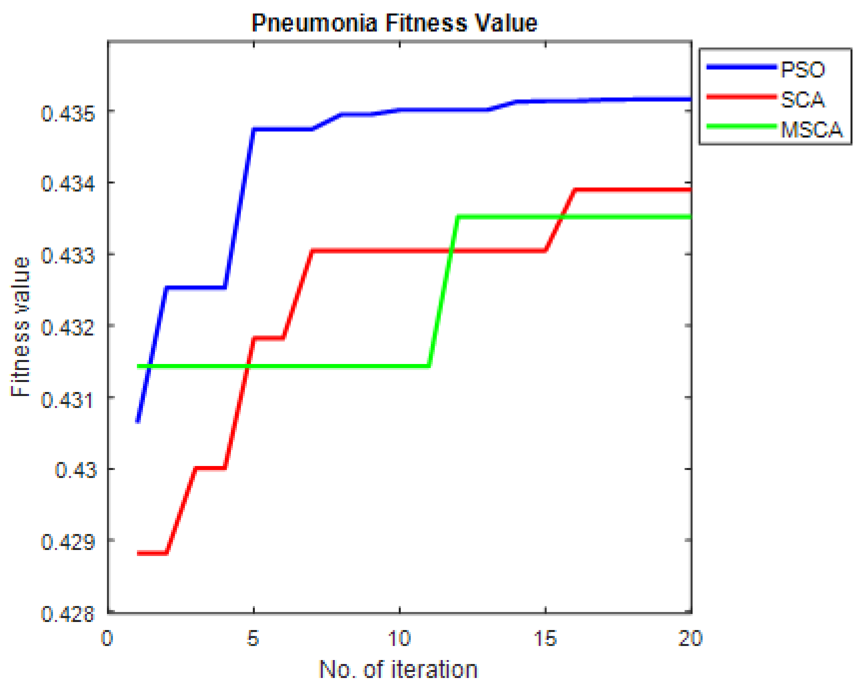

Fig.4.2 Lungs pneumonia image enhancement fitness Value by using PSO,SCA and MSCA

In fig. 4.2 shows the pneumonia lungs image enhancement and it is observed that the fitness value is nearly 0.4335 in the case of proposed MSCA optimization technique, which is less than in comparision to the PSO (0.4353) and SCA (0.4340) optimization technique around the 15th iteration. This indicate that the MSCA has bettter clarity of image enhacement than PSO & SCA in the case pneumonia lungs image also.

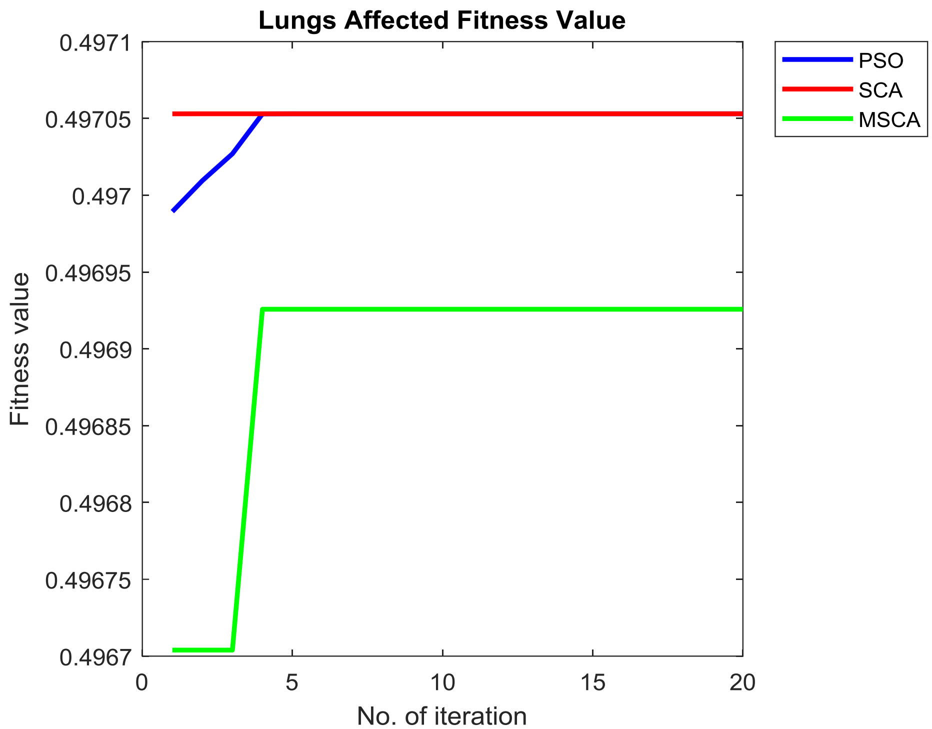

Fig.4.3 Lungs affected image enhancement fitness Value by using PSO,SCA and MSCA

In fig. 4.3 shows the affected lungs image enhancement and it is observed that the fitness value is nearly 0.49693 in the case of proposed MSCA optimization technique, which is less than in comparision to the PSO and SCA models have the same fitness value 0.49706 starting from the 4th iteration. This indicate that the MSCA has bettter clarity of image enhacement than PSO & SCA in the case affected lungs image.

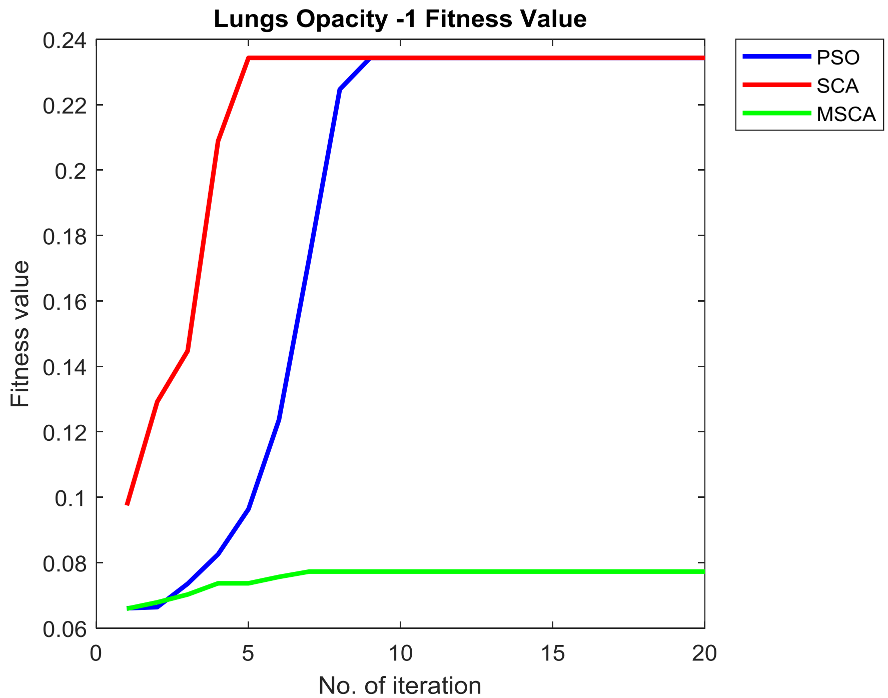

Fig.4.4 Lungs opacity image-1 enhancement fitness Value by using PSO,SCA and MSCA

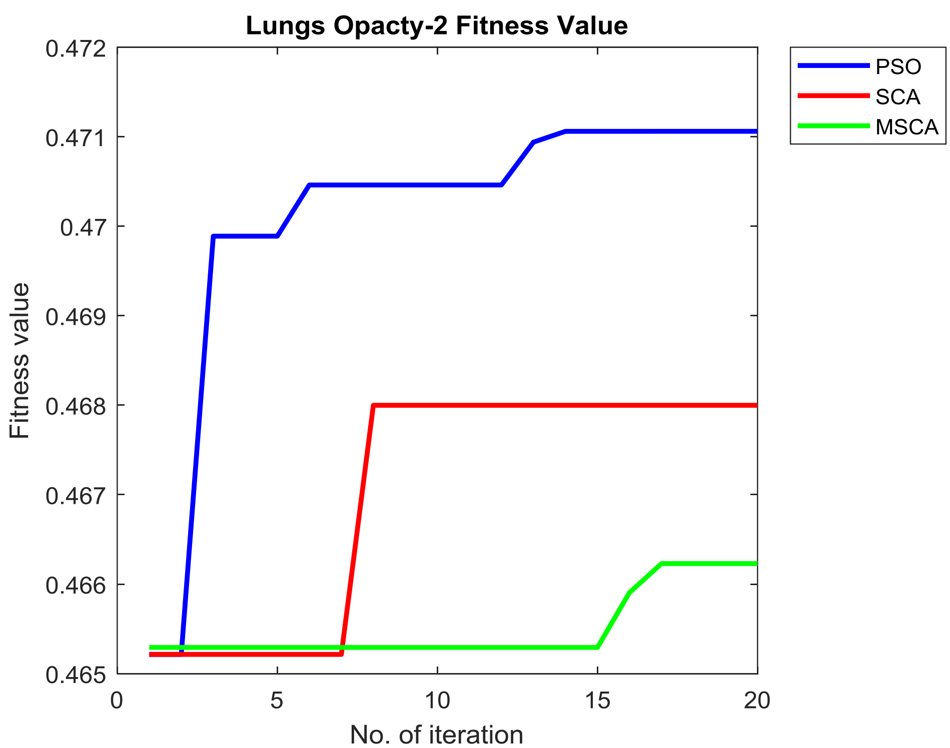

Fig.4.5 Lungs opacity image-2 enhancement fitness Value by using PSO,SCA and MSCA

In fig. 4.4 & 4.5 shows the lung opacity image-1 & image-2 enhancement and it is observed that the fitness value are nearly 0.075 & 0.4662 in the case of proposed MSCA optimization technique repectively, which is very less than in comparision to the PSO is 0.235 & 0.471 and SCA models has the fitness value 0.235 & 0.468 starting from the 8th iteration for image 1and 17th iteration for image-2. From both graphes, we learn that the MSCA has more bettter clarity of image enhacement than PSO & SCA in the case lungs opacity image.

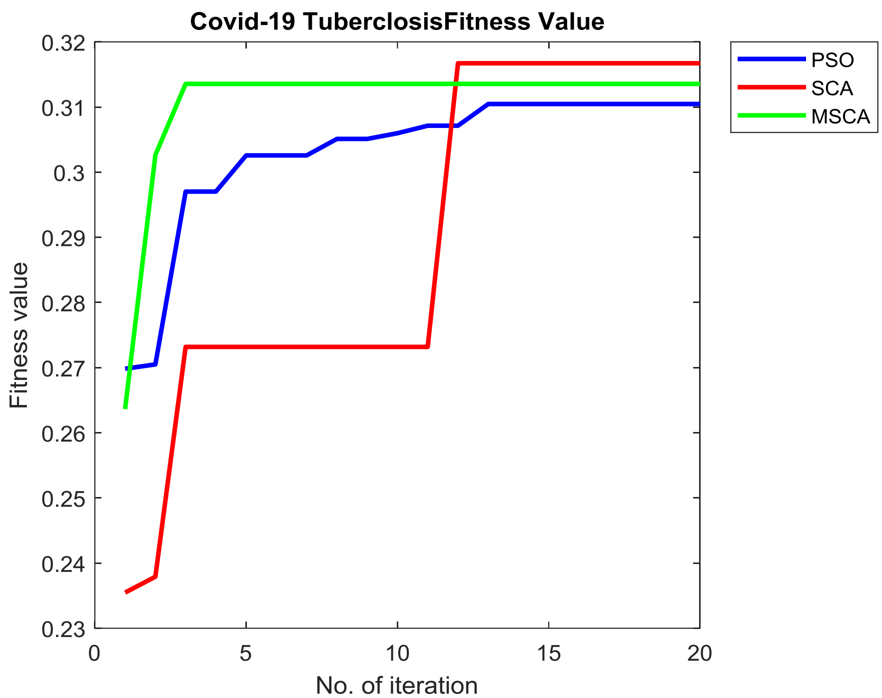

Fig.4.6 Lungs tuberclosis image-3 enhancement fitness Value by using PSO,SCA and MSCA

In this fig. 4.6 shows the tuberclosis lungs image enhancement and it is observed that the fitness value is nearly 0.314 in the case of proposed MSCA optimization technique, which is more than PSO and less than SCA model havng the fitness values 0.310 & 0.316 starting from the 14th iteration. This indicate that the MSCA has bettter clarity of image enhancement than SCA but less enhacement than PSO in the case tuberclosis lungs image.

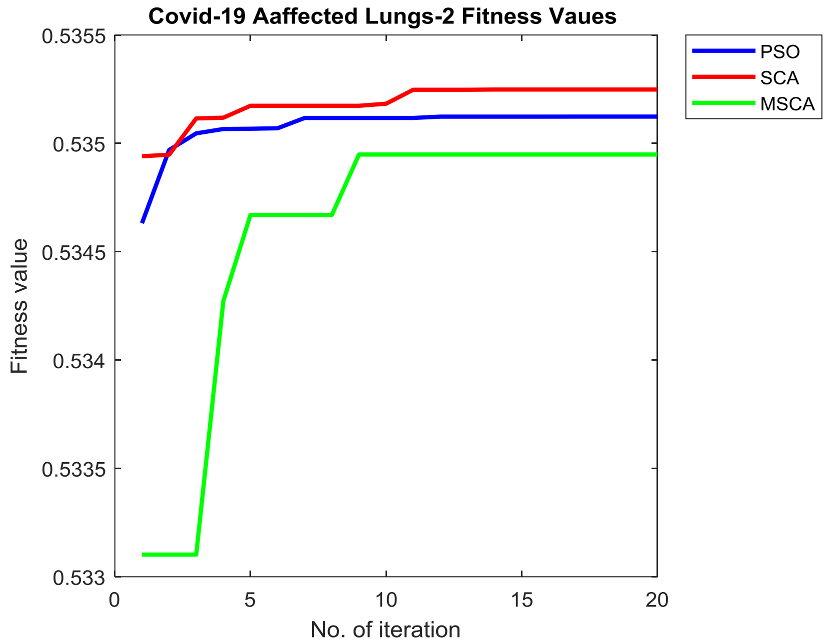

Fig.4.7 Lungs covid infected image enhancement fitness Value by using PSO,SCA and MSCA

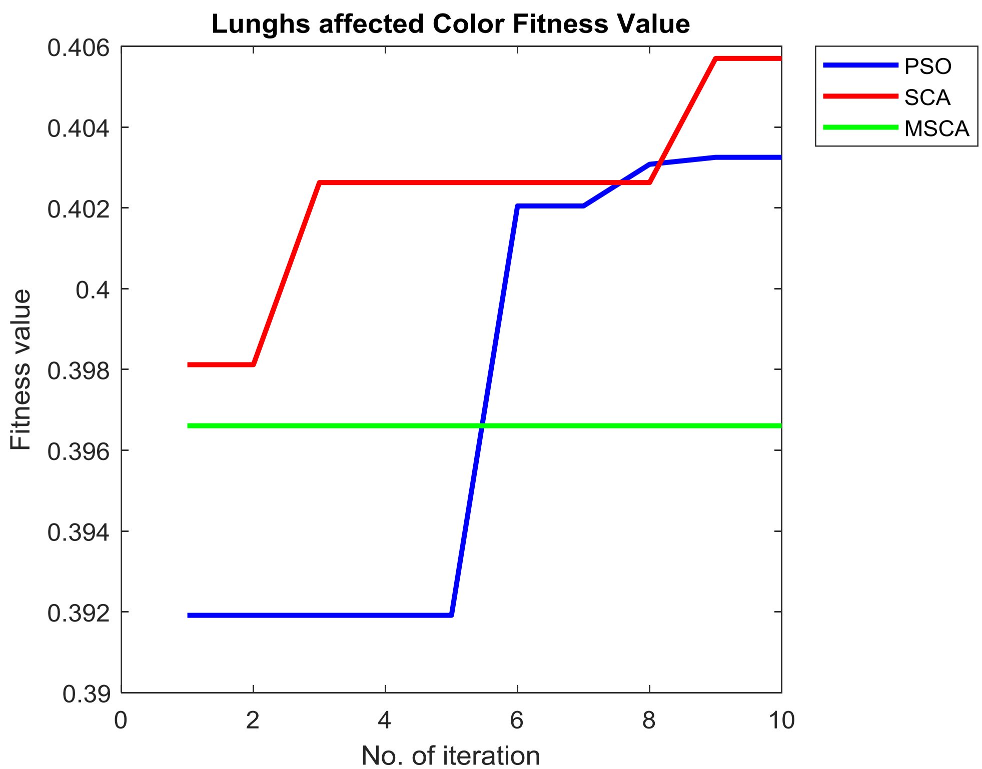

Fig.4.8 Lungs covid affected coloured image enhancement fitness Value by using PSO,SCA and MSCA

In figure 4.7 & 4.8 shown lung covid affected for grayscale & coloured image enhacement and the grayscale image fitness value is nearly 0.535 in proposed MSCA optimazation which is less than the fitness values of SCA & PSO models 0.5352 & 0.5353 repectively. For coloured image, the fitness value is constant for all iteration nealy 0.3965 of the proposed MSCA model but PSO & SCA have a fitness value 0.403 & 0.406 respectively. In both image the MSCA has better enhancement than PSO & SCA model.

The original x-ray images shown in figure 4.9 to 4.14 both gray & coloured images were enhanced using PSO, SCA and MSCA algorithm. The grayscale images are directly processed without changing color to gray.

Fig.4.9 Lung opacity enhanced image by utilizing PSO, SCA and MSCA

Fig.4.10 Bacrriol Pnemonia enhanced image by utilizing PSO, SCA and MSCA

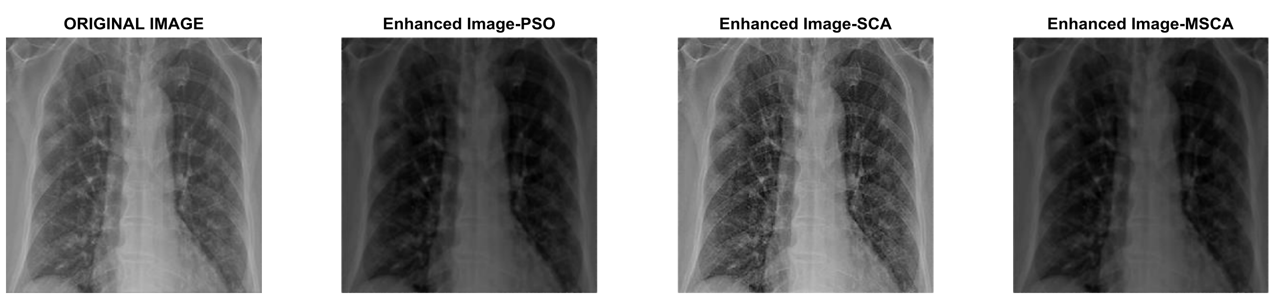

Fig.4.11 Pre-Pnemonia-1 enhanced image by utilizing PSO, SCA and MSCA

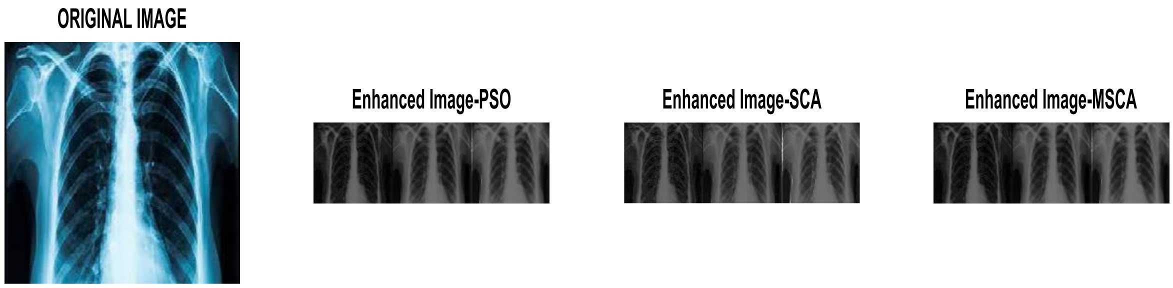

Fig.4.12 Pre-Pnemonia-2 enhanced image by utilizing PSO, SCA and MSCA

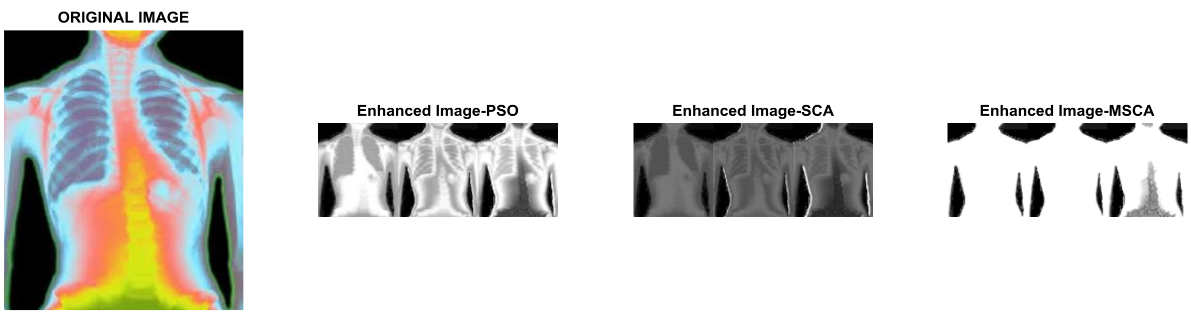

Fig.4.13 Lobar Pneumonia enhanced image by utilizing PSO, SCA and MSCA

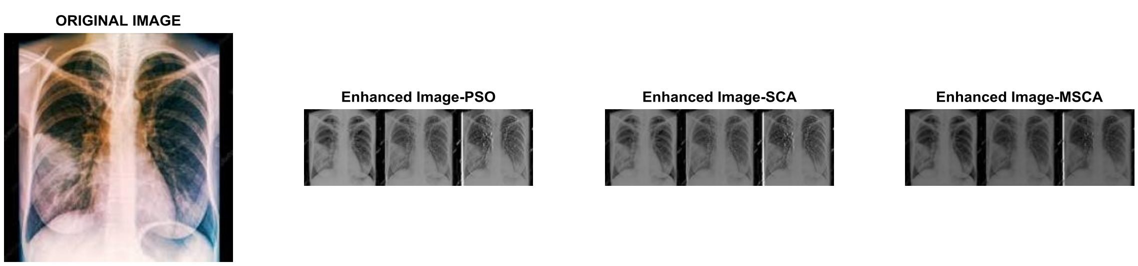

Fig.4.14 Lungs cancer enhanced image by utilizing PSO, SCA and MSCA

Figure 4.12 to 4.14 shows the original images are colured and converted all color to grayscale by only enhancing the luminance information. When the enhanced images are visualized, the images enhanced by MSCA are bettter clarity than the images enhanced by PSO& SCA models.

4.2 HOG Feature Descriptor results

Figure 4.15 to 4.19 shows the HOG feature of Covid affected-2, Lungs pre pnumonia, Lungs opacity, Lungs tuberclosis, Lungs covid infected enhanced images where the orientations of the different locations of the diseased region are clearly identified. Table 4.1 indicate the HOG feature exraction has better value than the other normalization parameters.

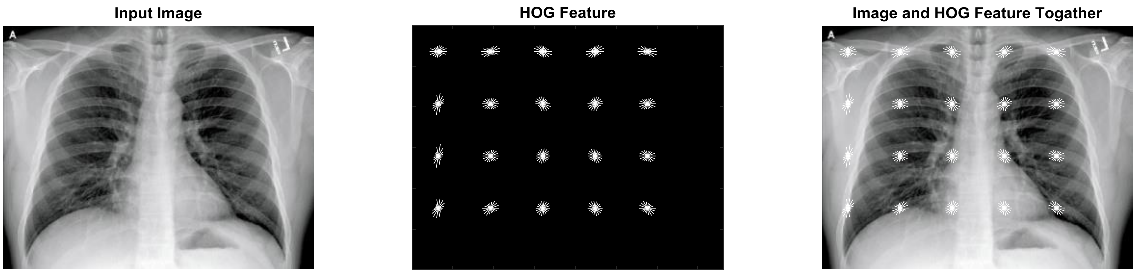

Fig.4.15 HOG feature of Bacrriol Pnemonia enhanced image.

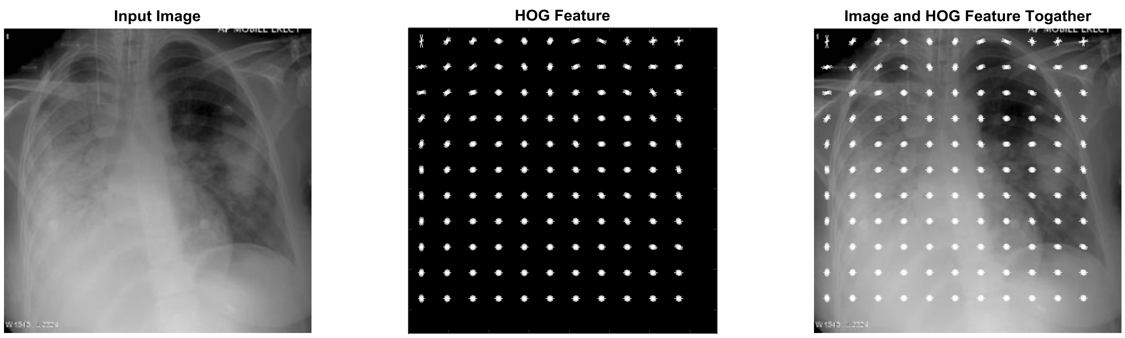

Fig.4.16 HOG feature of Lung opacity -1 enhanced image

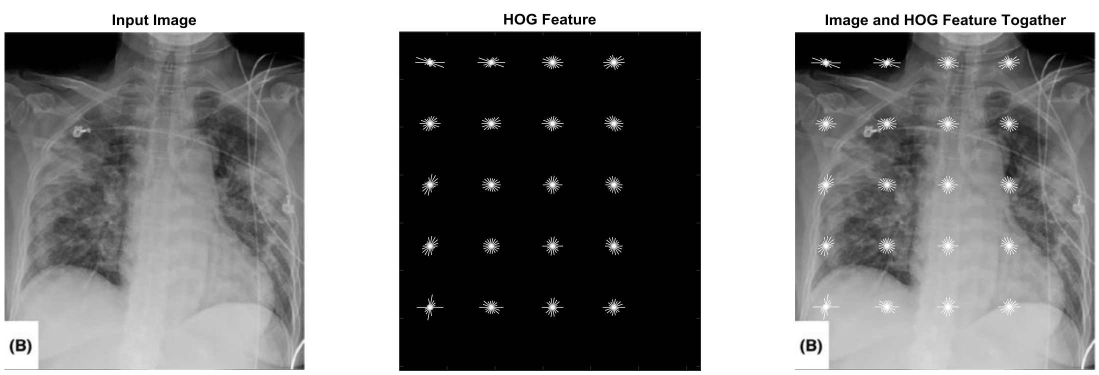

Fig.4.17 HOG feature of Covid affected-1 enhanced image

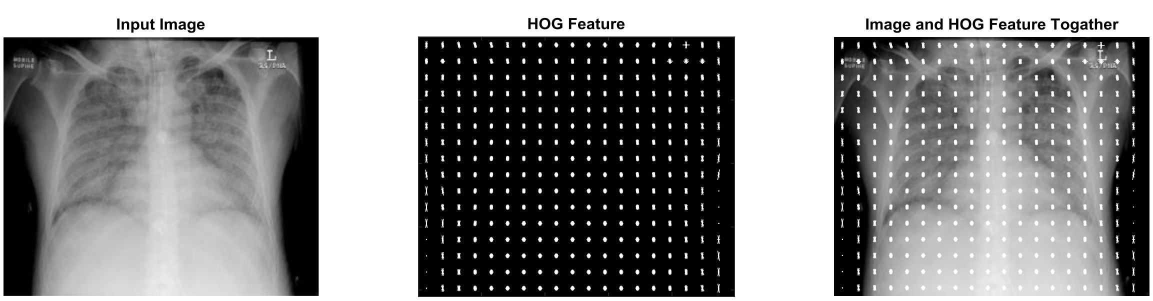

Fig.4.18 HOG feature of Covid affected-2 enhanced image

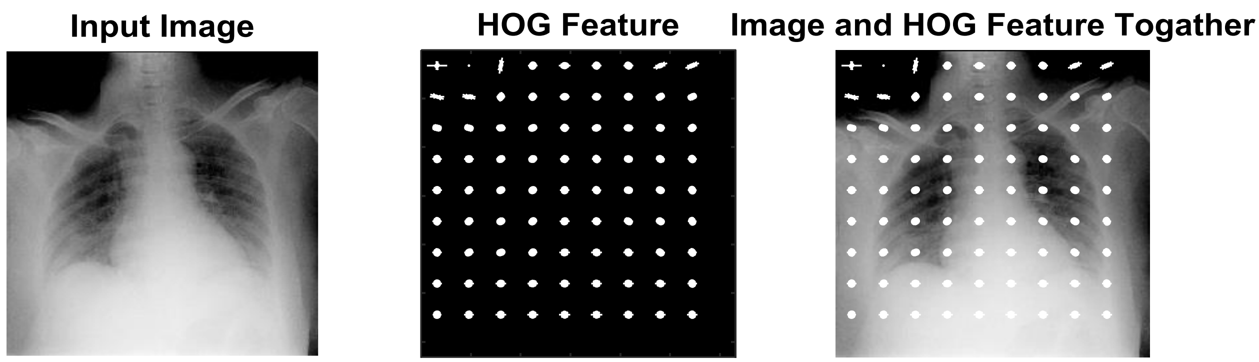

Fig.4.19 HOG feature of Pre-Pnemonia enhanced image

Table 4.1 Normalized feature extraction

Images	Correlation	DM	Coarseness	Skewness	HOG	Energy
Img-1	0.1233	0.1593	0.1322	0.3448	**0.9614**	0.2677
Img-2	0.1211	0.1416	0.3418	0.4282	**0.9641**	0.1454
Img-3	0.1084	0.0701	0.2503	0.2826	**0.9704**	0.1611
Img-4	0.1061	0.0552	0.2602	0.3703	**0.8127**	0.1458
Img-5	0.1309	0.0106	0.1928	0.3882	**0.8304**	0.1066

4.3 Segmentation Results

Fig. 4.20 to 4.28 presets the segmented images by utilizing the FCM,FGFCM, FLICM, FRFLICM segmentation techniques. It is found that the FRFLICM segmentation techniques outperformed in detection of the diseased regions minutely prest in the lungs chest x-ray image.

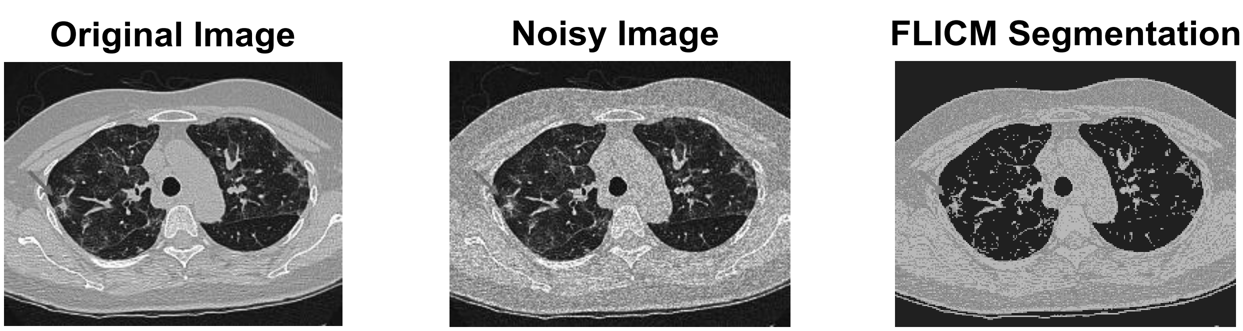

Fig.4.20 Pnemonia Segmented image by utilizing FLICM technique

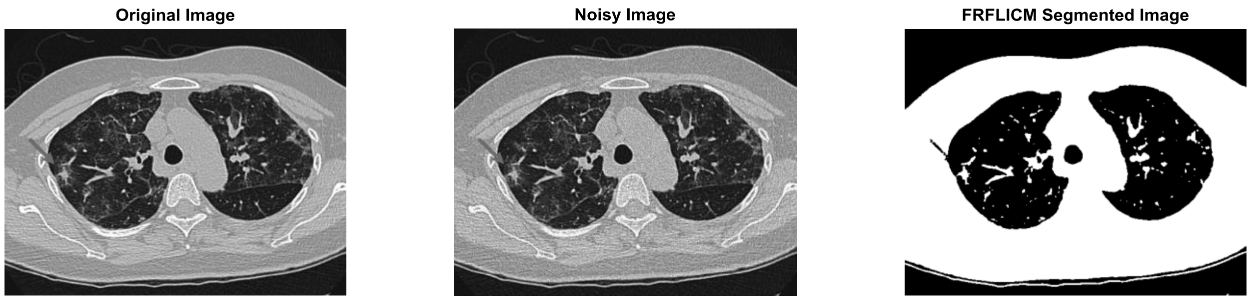

Fig.4.21 Pnemonia Segmented image by utilizing FRFLICM technique

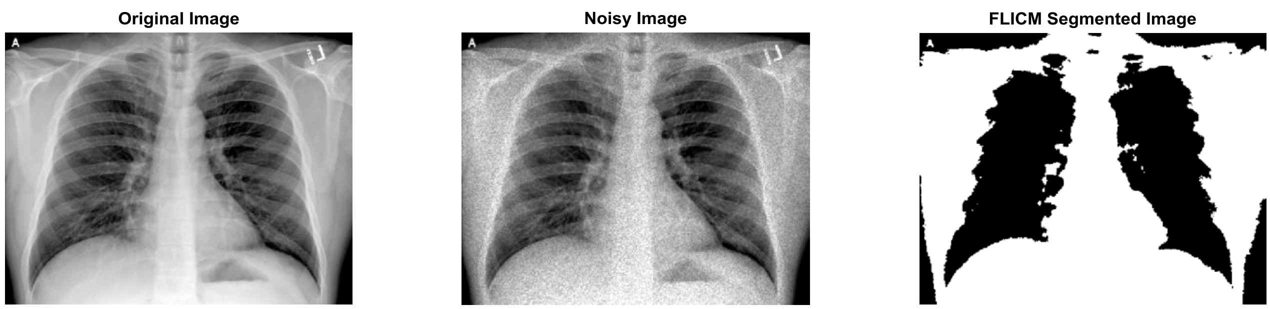

Fig.4.22 Pnemonia Segmented image by utilizing FLICM technique

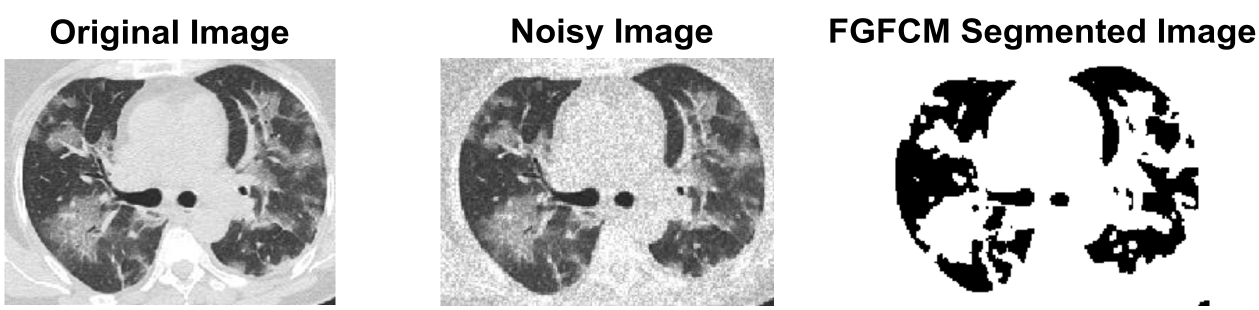

Fig.4.23 Lung opacity Segmented image by utilizing FGFCM technique

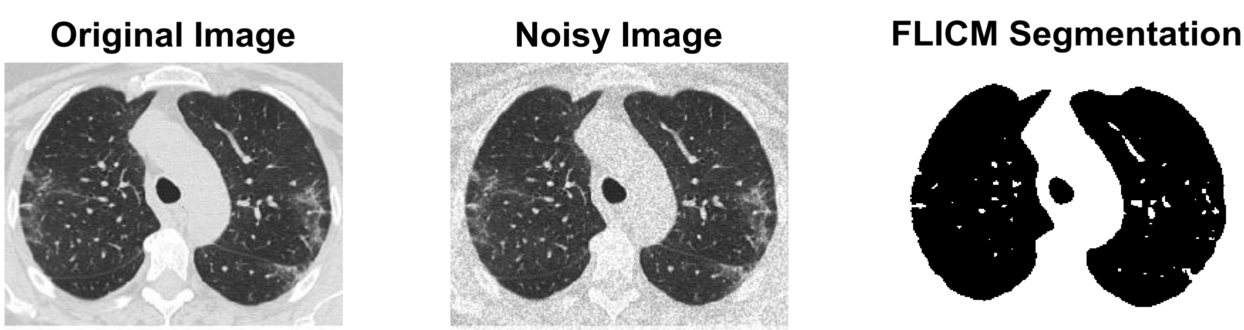

Fig.4.24 Lung opacity Segmented image by utilizing FLICM technique

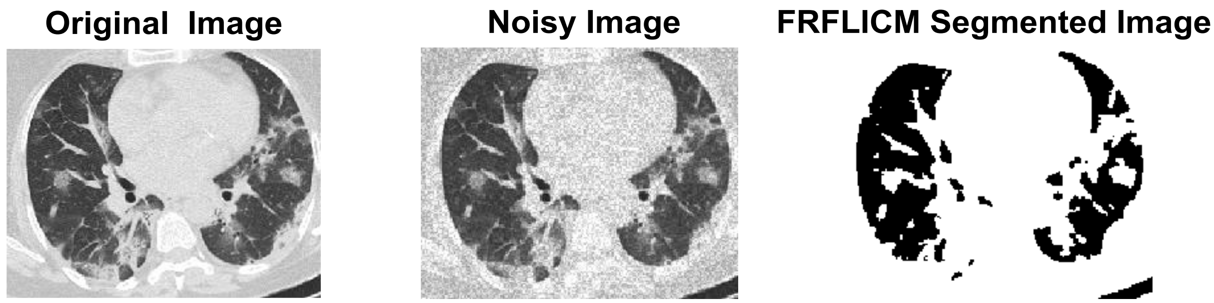

Fig.4.25 Lung opacity Segmented image by utilizing FRFLICM technique

Fig.4.26 Pnemonia Segmented image by utilizing FGFCM technique

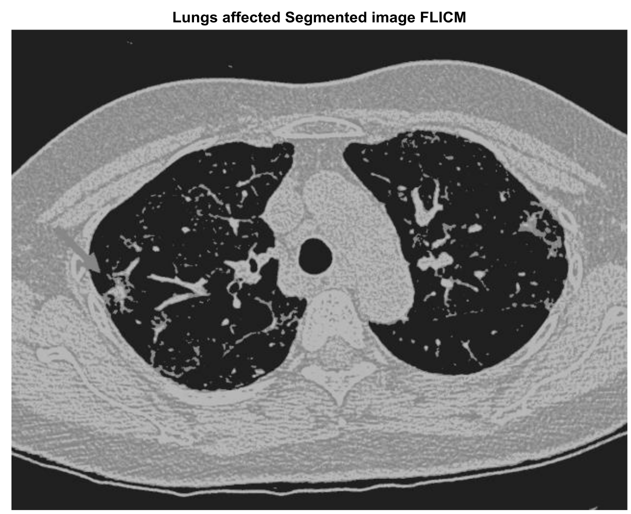

Fig.4.27 Pnemonia Segmented image by utilizing FLICM technique

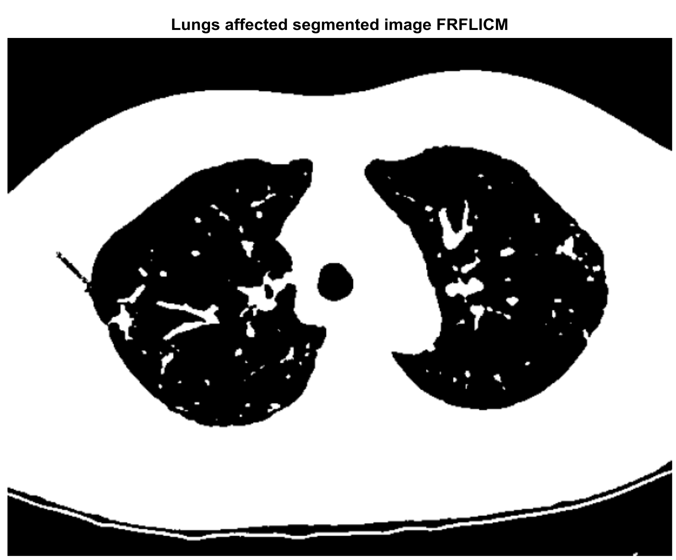

Fig.4.28 Pnemonia Segmented image by utilizing FRFLICM technique

4.3.1 PImage Segmentation Quality Measures

(1) Structured Similarity Index (SSIM) (Mishra et al., 2019) The Structural Similarity Index (SSIM) signifies losses in images. It is defined as

$$SSIM = \left(\frac{\sigma_{xy}}{\sigma_x \sigma_y}\right)\left(\frac{2\overline{x}\overline{y}}{\left(\overline{x}^2\right)+\left(\overline{y}^2\right)+C_1}\right)\left(\frac{2\sigma_x\sigma_y}{\left(\sigma_x\right)^2+\left(\sigma_y\right)^2+C_2}\right) \tag{4.1}$$

(2) Mean Square Error (MSE) (Mishra et al., 2019) The mean square error is defined for the image as

$$MSE = \frac{1}{P \times Q}\sum.\sum\left(f(x,y)-f^R(x,y)\right)^2 \tag{4.2}$$

(3) Peak Signal-to-Noise Ratio (PSNR) in dB(Mishra et al., 2019)**:** it is defined” as

$$PSNR = 20\log_{10}\frac{\left(2^n-1\right)}{MSE}db \tag{4.3}$$

Lower value of MSE and higher value of PSNR indicate better signal-to-noise ratio.

Table 4.2 Quality measures for the Lungs image with rician noise

Rician Noise				
	$\sigma_n = 10$		$\sigma_n = 20$	
Algorithm	**SSIM**	**PSNR(dB)**	**SSIM**	**PSNR(dB)**
FCM	0.7621	17.23	0.6912	15.35
FCM S1	0.7834	18.56	0.7146	16.88
FCM S2	0.7889	18.89	0.7621	17.12
En FCM	0.7982	23.02	0.7813	18.87
FGFCM	0.8349	27.78	0.8182	26.14
FLICM	0.8731	31.58	0.8248	29.41
FRFLICM	**0.9878**	**35.26**	**0.9129**	**34.29**

The proposed FRFLICM technique with rician noise model shows a better performance of noise reduction. The comparison of the different algorithms and two quality indexes are Structural

Similarity (SSIM) index and PSNR (Peak signal to noise ratio) (Mishra et al., 2019) are considered. SSIM is more subtle to the noise in the images.

Table 4.3 Segmentation Accuracy

Algorithm	Noise level	
	Rician Noise ($\sigma_n = 10$)	Rician Noise ($\sigma_n = 20$)
FCM	92.38	89.19
FCM S1	97.53	90.14
FCM S2	98.91	94.62
En FCM	98.83	97.82
FGFCM	98.87	97.01
FLICM	98.92	98.61
FRFLICM	**99.26**	**98.93**

The segmentation accuracy in the proposed FRFLICM IS 99.26% and 98.93 % when $\sigma_n = 10$ and $\sigma_n = 20$. Even though the FLICM is showing better segmentation accuracy, but FRFLICM is preferable for the chest images. The segmentation accuracy of different segmentation techniques are presented in Table 4.2.

4.4 Classification Results

4.4.1 Performance Measure of classifiers

For our experiment, we have considered dataset having different types of lungs diseased images. The performance measures are considered in this research as computational time, sensitivity, specificity and accuracy. The total of 3000 data are considered for the classification task. Out of which 80% of the data are considered for training and 20% of the data are considered for validation. We have considered 5×5 cross validation procedure to evade over fitting problem. The classification performance is presented in Table-4.4.

$$Sensitivity = TPR = \frac{TP}{TP+FN} \quad Specificity = TNR = \frac{TN}{TN+FP} \quad Accuracy = \frac{TP+TN}{TP+TN+FP+FN}$$

Table-4.4 Performance Evaluation of Classifiers

Model	No. of data	Computational Time in sec	Sensitivity in %	Specificity in %	Accuracy in %
SVM	3000	98.4839	95.65	95.58	96.85
ELM	3000	65.3782	97.13	96.78	97. 78
SCA-ELM	3000	34.2569	97.45	98.39	**97.32**
MSCA-ELM	3000	24.1128	**98.78**	**99.23**	**99.24**

Table 4.5 5×5-fold validation during each run

	Fold1	**Fold2**	**Fold3**	**Fold4**	**Fold5**	**Total**	**Accuracy (%)**
Run-1	100	98	100	100	100	498	**99.6**
Run-2	100	100	98	99	100	497	99.4
Run-3	98	100	98	100	99	494	98.8
Run-4	100	98	98	99	99	494	98.8
Run-5	100	100	100	98	100	498	99.6
Final result							**99.24**

Accuracy in percentage = [99.6+99.4+98.8+98.8+99.6]/5=99.24

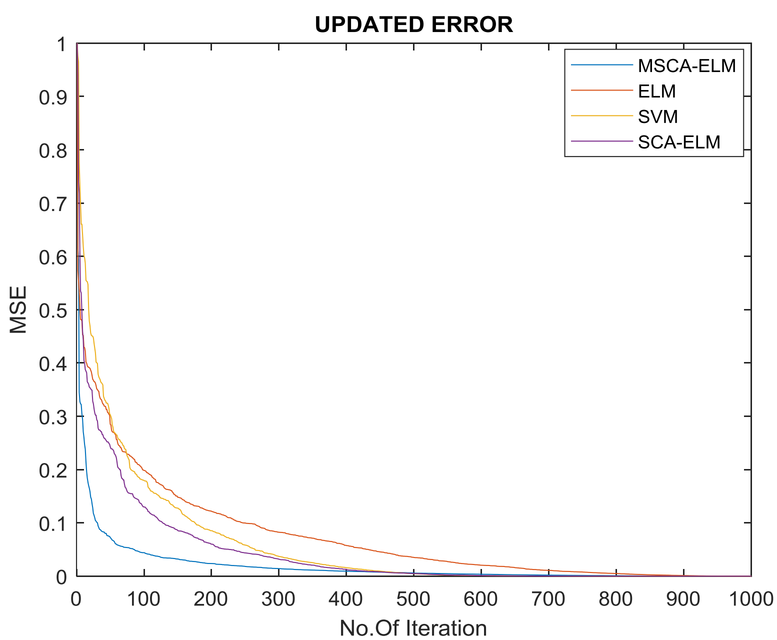

Fig.4.29 Mean square results obtained by SVM, ELM, SCA-ELM and MSCA-ELM

The X axis of this graph representes the simulation number of iteration and the Y axis determines the MSE in percentage. The proposed MSCA –ELM graph was the blue line steadly approaching convergence at 380 iterations. Whereas the graphs were red, golden and pink lines, steadly approaching convergence at 850, 510 and 450 iterations respectively.

4.5 Summary of Discussion

Fig. 4.1 to 4.8 shows the fitness values of the lungs image enhancement by using PSO,SCA and MSCA for the Lungs pneumonia, Lungs affected cancer Lungs pre pnumonia, Lungs opacity, Lungs tuberclosis, Lungs covid infected lungs related diseases. It is visualised from the fitness values that the better clarity of enhancement images leads in the case of the proposed MSCA-ELM model. Fig. 4.9 to 4.14 shows the enhanced image results of Lungs pneumonia, Lungs affected cancer Lungs pre pneumonia, Lungs opacity, Lungs tuberclosis, Lungs covid infected lungs related diseases by utilizing PSO, SCA and MSCA models. Fig. 4.15 to 4.19 shows the HOG feature of Covid affected-2 , Lungs pre pnumonia, Lungs opacity, Lungs tuberclosis, Lungs covid infected enhanced images where the orientations of the different locations of the diseased region are identified. The segmentation accuracy is presented in the table 4.3. It is found that the segmentation accuracy is 99.26 % in the case of FRFLICM in comparison to the other FLICM, FGFCM etc., Techniques. Table 4.2 "shows the experimental results for two different values of racian noise. It is also observed that when; the quality measure PSNR value is 35.26 dB and 34.29 dB in case of proposed FRFLICM and FLICM segmentation techniques respectively. The higher value of PSNR in case of FRFLICM indicate better signal-to noise ratio in the extracted image. Also the larger value of SSIM indicates the noise reduction in the extracted image which is presented in Table 4.2". Table 4.2 shows the Quality measures for the Lungs images with rician noise of standard deviation of $\sigma_n = 10$ and $\sigma_n = 20$. The quality measure SSIM and PSNR shows the noise reduction capability of the FRFLICM segmentation technique. Computational time plays a significant role for evaluation of a classifier. At first, the computation time of each stage of the proposed MSCA-ELM method is calculated, and finally the average value is calculated as 24.1128 sec lungs dataset. Further the computation time for SVM, ELM, SCA-ELM and MSCA-ELM for each stage has been calculated and the average value is obtained as 98.4839 seconds, 65.3782seconds, 34.2569 seconds and 24.1128 seconds. It is observed that the proposed MSCA-ELM method outperforms than the other mentioned algorithms. The mean squared error (MSE) value shown in Fig.4.29. It is found that the proposed MSCA- ELM is improved than other classifiers in terms of sensitivity, specificity and accuracy. Table 4.4 shows the performance measure of all classifiers. The 5x5-fold cross validation procedure have been employed for all the algorithms using lungs x-ray chest dataset. The accuracy obtained with SVM, ELM, SCA-ELM and MSCA-ELM are as 98.78%, 99.23%, and 99.24% respectively. The cross validation is itemized in Table 4.5. The MSCA-ELM model is modest in structure and free from multifaceted mathematical calculations in comparison to supplementary methods. Fig.4.29 shows the mean square error comparison of all the mentioned classification models. It is also found that SVM, ELM, and SCA ELM models took 850, 510 and 450 iterations respectively. But, the proposed MSCA-ELM took 380 iterations to converge, which displays the toughness of the proposed model. The classification accuracies are presented in the Table 4.4.

CHAPTER-5

CONCLUSION AND RECOMMENDATION

5.1 Conclusion

The research work offered a novel image enhancement technique, segmentation technique and Modified SCA-ELM classification model for lungs related diseases form the Chest X-Ray Images. At the first instance the image enhancement technique has been proposed by utilizing the modified SCA a meta-heuristic algorithm and the proposed image enhancement technique has been compared with the conventional SCA and PSO optimization algorithm. The proposed modified Image enhancement technique results are show the noise reduction capability to some extent and smoothen the images. The enhanced images are under gone the segmentation to detect the lungs diseased regions from the images. The FRFLICM segmentation technique has been proposed to detect the diseased regions and the results are presented in the results section. Further the HOG features are extracted from the images and to locate the diseased regions and the features are utilized for classification and error calculation.

The proposed modified SCA -PSO algorithm has been utilized for weight optimization of ELM model. The features are also fed to the proposed ELM, SVM, SCA-ELM classifier models to validate the robustness of the classifier. The proposed comparison results with the proposed Modified SCA-PSO based ELM models are presented. The performance measure sensitivity, specificity and accuracy are presented in the results section as 98.78%, 99.23%, and 99.24% respectively. Even though the computational time is approximate to the SCA-ELM model, but the accuracy in terms of classification is better obtained by the proposed modified SCA-PSO based ELM model. The proposed modified SCA-PSO based ELM model has shown decent potentiality of classifying the lungs disease in comparison to the conventional models.

5.2 Future work and recommendation

The proposed MSCA image enhancement, FRFLICM segmentation and modified SCA-ELM classifier models can be applied for breast cancer, liver tumor, Brain tumor etc., for further study

REFERENCES

American Lung Association -Learn about lung disease symptoms, causes and treatments, as well as advice for recognizing and managing lung diseases. April 14, 2021.

Ahmed I. H., et al., (2016). "Sine Cosine Optimization Algorithm for Feature Selection", IEEE. DOI: 10.1109/INISTA.2016.7571853.

Ahmed M.N., Yamany SM., Mohamed N., Farag A.A. and Moriarty T. (2002)."A modified fuzzy c-means algorithm for bias field estimation and segmentation of MRI data". IEEE Trans Med Imaging 21(3):193– 199. https://doi.org/10.1109/42.996338

Athanasios V., Eftychios P., Iason K., Anastasios D. and Nikolaos D., (2021). "A Few-Shot U-Net Deep Learning Model for COVID-19 Infected Area Segmentation in CT Images", Molecular Diversity Preservation International.

Alzahrani A., Amin B., and Fahima A., (2022). "Detecting COVID-19 Pneumonia over Fuzzy Image Enhancement on Computed Tomography Images" Computational and Mathematical Methods in Medicine Volume. https://doi.org/10.1155/2022/1043299

Athanasios V., Eftychios P., Iason K., Anastasios D., and Nikolaos D., (2020). "Deep learning models for COVID-19 infected area segmentation in CT images", cold spring harbor laboratory,. https://doi.org/10.1101/2020.05.08.20094664

Behera S. K, Mishra S., Rana D., (2015) "Image enhancement using accelerated particle swarm optimization", Int J Eng Res Technol 4 :1049–1055.

Cai W., Chen S., and Zhang D., (2007). "Fast and robust fuzzy c-means clustering algorithms incorporating local information for image segmentation". Pattern Recognit 40(3):825–838,. https://doi.org/10.1016/j.patcog.2006.07.011

Chen S., and Zhang D. (2004) "Robust image segmentation using FCM with spatial constraints based on new kernel-induced distance measure". IEEE Trans System Man Cybern B Cybern 34(4):1907–1916. https://doi.org/10.1109/tsmcb.2004.831165.

Deepa S. N and Arunadevi B., (2013). "Extreme learning machine for classification of brain tumor in 3D MR images". Informatologia 46(2):111–121. ISSN 1330-0067

Ding Y. and Fu X. (2016). "Kernel-based fuzzy c-means clustering algorithm based on genetic algorithm". Neurocomputing, 188:233–238. https://doi.org/10.1016/ j.neucom.2015 .01. 106

Harmon S. A. et al., (2020) "Artificial intelligence for the detection of COVID-19 pneumonia on chest CT using multinational datasets", nature communications,. https://doi.org/10.1038/s41467-020-17971-2

Krinidis S., and Chatzis V., (2010). “A robust fuzzy local information c-means clustering algorithm”. IEEE Trans Image Process, 19(5):1328– 1337. https://doi.org/10.1109/ tip. 2010.2040763 AQ7

Kumar P., & Vijayakumar B., (2015). “Brain Tumor MR Image Segmentation and Classification Using by PCA and RBF Kernel Based Support Vector Machine”. Middle-East Journal of Scientific Research, 23(9), 2106-2116.

Lu S., Lu Z., and Zhang Y., (2018). “Pathological Brain Detection based on AlexNet and Transfer Learning’’, Journal of Computational Science. https://doi.org/10.1016/j.jocs. 2018.11.008

Matthew Z. and Adam K., (2020).“Classification of Lung Diseases Using Deep Learning Models”, Springer Nature Switzerland, pp. 621–634. https://doi.org/10.1007/978-3-030-50420-5_47

Mishra S., Sahu P.&. Senapati M. R, (2019) “MASCA- PSO based LLRBFNN Model and Improved fast and robust FCM algorithm for Detection and Classification of Brain Tumor from MR Image” Evolutionary Intelligence, ISSN 1864-5909, Springer https://doi.org/10.1007/s12065-019-00266-x,July,2019.

Mishra S., Gelmecha D. J., Ram Singh S., Rathee D. S. and Gopikrishna T., (2021) “Hybrid WCA–SCA and modified FRFCM technique for enhancement and segmentation of brain tumor from magnetic resonance images”, Biomedical Engineering: Applications, Basis and Communications, Vol. 33, No. 3. DOI: 10.4015/S1016237221500174.

Morens D. M, Folkers G. K, and Fauci A. S, (2022) “The Concept of Classical Herd Immunity May Not Apply to COVID-19”, Journal of Infectious Diseases. https://doi.org/10.1093/infdis/jiac109

Mohd Fauzi B. O., and Noramalina B. A., (2011). “MRI Brain Classification using Support Vector Machine,” IEEE. DOI**:** 10.1109/ICMSAO.2011.5775605.

Mustafa G., et al., (2021) “Deep Convolutional Neural Network–Based Computer-Aided Detection System for COVID-19 Using Multiple Lung Scans: Design and Implementation Study”, Journal Of Medical Internet Research. doi: 10.2196/27468

Prudhvi V. N. and Venkateswarlu T., (2012). “Denoising of Poisson and Rician Noise from Medical Images using Variance Stabilization and Multiscale Transforms” International Journal of Computer Applications, Volume 57, No. 21.

Pedro S., et al.’, (2020).“COVID-19 detection in CT images with deep learning: A voting-based scheme and cross-datasets analysis”, Informatics in Medicine Unlocked, V. 20. https://doi.org/10.1016/j.imu.2020.100427

Robert D.N. (1999). “Wavelet-Based Rician Noise Removal for Magnetic Resonance Imaging” IEEE Transactions on Image Processing, Vol. 8, No. 10.

Rezaei K., and Agahi H., (2017). “Malignant and benign brain tumor segmentation and classification using SVM with weighted kernel width”. Sig Image Proc Int J (SIPIJ). https://doi.org/10.5121/sipij.2017.8203

Rahman M.M., Nooruddin S., Azharul K. M. and Dey N. K., (2021). “HOG + CNN Net: Diagnosing COVID‑19 and Pneumonia by Deep Neural Network from Chest X‑Ray Images” SN Computer Science. Doi: 10.1007/ s42979-021-00762-x

Seyedali M., (2016). “SCA: A Sine Cosine Algorithm for Solving Optimization Problems”, Knowledge-Based Systems. doi: 10.1016/j.knosys.2015.12.022

Salehi S., Abedi A., Balakrishnan S., and Gholamrezanezhad A., (2020) “Coronavirus disease 2019 (COVID-19): a systematic review of imaging findings in 919 patients” American Journal of Roentgenology.; 215(1):87–93. https:// doi. org/ 10. 2214/ AJR. 20. 23034

Shui-Hua W., Xiaosheng W., Yu-Dong Z., Chaosheng T., and Xin Z., (2020). “Diagnosis of COVID-19 by Wavelet Renyi Entropy and Three-Segment Biogeography-based Optimization”, International Journal of Computational Intelligence Systems, Volume 13, Issue 1, Pages 1332 – 1344. https://doi.org/10.2991/ijcis.d.200828.001

Shui-Hua W., Vishnu V. G., Juan M. G., Xin Z., and Yu-Dong Z., (2020). “Covid-19 Classification by FGCNet with Deep Feature Fusion from Graph Convolutional Network and Convolutional Neural Network”, Information Fusion Journal. DOI: 10.1016/j.inffus.2020.10.004

Shayan H., Mohsen A. , and Abbas S., (2020) “Diagnosis and detection of infected tissue of COVID-19 patients based on lung x-ray image using convolutional neural network approaches”, Elsevier Ltd. https://doi.org/10.1016/j.chaos.2020.110170.

Sun Y.F., Liang Y.C., Zhang W.L., Lee H.P, and Lin W.Z., (2005). “Optimal partition algorithm for the RBF neural network for financial time series forecasting”, In: Neural Comput. Appl, Vol. 14, No. 1, pp. 36-44.

Sonu S., and Mohan S. L.,(2015). “Automatic brain tumor detection and classification using svm classifier”. In: Proceedings of ISER 2nd international conference, Singapore;. p. 55-59.

Szilagyi L., Benyo Z., Szilagyii S. M, and Adam H.S, (2003) .“MR brain image segmentation using an enhanced fuzzy c-means algorithm”. In: Proceeding of the 25th annual international conference of the IEEE EMBS, pp 17–21.

Soria-Olivas E., et al. (2011). “BELM: Bayesian extreme learning machine,” IEEE Trans. Neural Netw., vol. 22, no. 3, pp. 505–509.

Tipping M. E.,(2001) “Sparse Bayesian learning and the relevance vector machine,” J. Mach. Learn. Res., vol. 1, pp. 211–244.

Uboho V., Xishuang D., Xiangfang L., Pamela O., and Lijun Q.,(2020) “Effective COVID-19 Screening using Chest Radiography Images via Deep Learning”, IEEE conference. 10.1109/MCNA50957.2020.9264294.

Vong C. M, and Won P. K., (2013). “A new framework of simultaneous-fault diagnosis using pairwise probabilistic multi-label classification for time-dependent patterns,” IEEE Trans. Ind. Electron., vol. 60, no. 8, pp. 3372–3385.

World Health Organization (WHO), webpage. https://www.who.int/emergencies/ diseases/novel-coronavirus-2019

Xiang Y., Shui-Hua W., Xin Z., and Yu-Dong Z., (2020)“ Detection of COVID-19 by GoogLeNet-COD”, computer science journal.

Xianwei J., C. Liang, and Z. Yu-Dong, (2020). “Classification of Alzheimer’s disease via Eight-Layer Convolutional Neural Network with Batch Normalization and Dropout Techniques”, Journal of Medical Imaging and Health Informatics, Volume 10, Number 5, pp. 1040-1048(9) https://doi.org/10.1166/jmihi.2020.3001.

Yu-Dong Z., Chaosheng T., and Junding S., (2018) “Multiple sclerosis identification by convolutional neural network with dropout and parametric ReLU”, Journal of Computational Science, V. 28, P 1-10. https://doi.org/10.1016/j.jocs.2018.07.003.

Yu-Dong Z., Suresh C. S, Li-Yao Z., Juan M. G., and Shui-Hua W. , (2020) “A seven-layer convolutional neural network for chest CT based COVID-19 diagnosis using stochastic pooling”, IEEE Sensors Journal. DOI: 10.1109/JSEN.2020.3025855

Yu-Dong Z., Deepak R. N., Xin Z., and Shui-Hua W., (2020). “Diagnosis of secondary pulmonary tuberculosis by an eight-layer improved convolutional neural network with stochastic pooling and hyper parameter optimization”, Journal of Ambient Intelligence and Humanized Computing. https://doi.org/10.1007/s12652-020-02612-9.

Yu-Dong Z., Chichun P., Xianqing C., and Fubin W., (2018). “Abnormal breast identification by nine-layer convolutional neural network with parametric rectified linear unit and rank-based stochastic pooling”, Journal of Computational Science. DOI: 10.1016/j.jocs.2018.05.005

.